The role of aneuploidy in the evolution of cancer drug resistance

Remus Stana[1], Uri Ben-David[2], Daniel B. Weissman[3], and Yoav Ram[1,*]

[1]School of Zoology, Faculty of Life Sciences, Tel Aviv University, Tel Aviv, Israel
[2]Department of Human Molecular Genetics and Biochemistry, Faculty of Medicine, Tel Aviv University, Tel Aviv, Israel
[3]Department of Physics, Emory University, Atlanta, GA
[*]Corresponding author: yoav@yoavram.com

November 25, 2023

Abstract

Evolutionary rescue is the process by which a population is able to survive a sudden environmental change which initially causes the population to decline towards extinction. A prime example of evolutionary rescue is the ability of cancer to survive being exposed to various treatments. We are interested in the mechanisms through which a population of cancer cells are able to adapt to chemotherapy, and in particular, the role played by chromosomal instability (aneuploidy). Cancer cells which have aneuploidy are hypothesized to have a higher fitness in an environment altered by anti-cancer drugs as they have incomplete pathways which drugs activate in order to kill the cells. Aneuploidy is highly prevalent in tumors and certain drugs which attempt to combat cancers through increasing chromosomal instability. As a result, the question we wish to answer is how aneuploidy impacts the fate of the population of cancer cells. We propose to model evolutionary rescue with the help of multi-type branching processes to obtain the probability that cancer will survive. We obtain analytic expressions for the probability of evolutionary rescue as a function of the initial tumor size, the growth rates of the different cancer genotypes and observe that aneuploidy plays an important role in the survival of the cancer cell population when the initial tumor size is not too large and the effect of the anti-cancer drug on the aneuploid cells is not too severe.

Introduction

Aneuploidy in cancer. Chromosomal instability (CIN) is the mitotic process in which cells suffer from chromosome mis-segregation that leads to aneuploidy, where cells are characterized by structural changes of the chromosomes and copy number alterations (Schukken and Foijer, 2018). Interestingly, aberrations in chromosome copy number have been shown to allow cancer cells to survive under stressful conditions such as drug therapy (Lukow et al., 2021, Rutledge et al., 2016). Indeed, cancer cells are often likely to be aneuploid, and aneuploidy is associated with poor patient outcomes (Ben-David and Amon, 2020).

The role of chromosomal instability (CIN) in the emergence of cancer has been studied extensively in the past decades (Christine et al., 2018, Komarova et al., 2003, Michor et al., 2005, Nowak et al., 2002, Pavelka et al., 2010, Zhu et al., 2018). One hypothesis is that CIN facilitates tumor genesis by accelerating the removal of tumor suppression genes (TSG) and subsequent appearance of cancer. The deletion of tumor suppression genes can happen in two ways: two point mutations deleting both alleles of the TSG (assuming a diploid genotype), or one point mutation and one chromosomal loss event. Initial theoretical studies have shown that aneuploidy can have a significant role in the deletion of the the tumor suppressing genes when compared to two consecutive point mutations (Komarova et al., 2008, 2003, Michor et al., 2005, Nowak et al., 2002). However, when taking into account that the appearance of aneuploidy requires a mutation to trigger CIN, the probability that CIN precedes tumor genesis is highly unlikely (Komarova and Wodarz, 2004).

Evolutionary rescue. Populations adapted to a certain environment are vulnerable to environmental changes, which might cause extinction of the population. Examples of such environmental changes include climate change, invasive species or the onset of drug therapies. Adaptation is a race against time as the population size decreases in the new environment (Tanaka and Wahl, 2022). *Evolutionary rescue* is the process where the population acquires a trait that increases fitness in the new environment such that extinction is averted. It is mathematically equivalent to the problem of crossing of fitness valley (Weissman et al., 2009, 2010). There are three potential ways for a population to survive environmental change: migration to a new habitat similar to the one before the onset of environmental change (Cobbold and Stana, 2020, Harsch et al., 2014, Zhou, 2022); adaptation by phenotypic plasticity without genetic modification (Carja and Plotkin, 2017, 2019, Levien et al., 2021); and adaptation through genetic modifications, e.g., mutation (Orr and Unckless, 2014, Uecker and Hermisson, 2011, 2016, Uecker et al., 2014).

Models of evolutionary rescue usually assume that the fitness of the wildtype and mutant are homogeneous in time. An exception was given by Marrec and Bitbol (2020), who modeled the fitness of the wildtype and mutant as time dependent. Evolutionary rescue in a quasi-periodic environment has been investigated by Marrec and Bank (2023) with the observation that stochasticity increases the chance of extinction in comparison to the case with deterministic environmental fluctuations. Additionally, Uecker and Hermisson (2011) investigated the probability of fixation of a beneficial mutation in a variable environment with arbitrary time-dependent selection coefficient and population size. Most models focus on the probability that at least one mutation rescues the population. How multiple mutations contribute to the survival of the population is less explored, but Wilson et al. (2017) have shown that evolutionary rescue is significantly enhanced by soft selective sweeps when multiple mutations contribute. Additionally, including a range of possible alleles with different fitness which could avert extinction has been coupled with Fischer's geometric model to analyze the probability of evolutionary rescue (Martin et al., 2007, Osmond et al., 2020, Wahl and Campos, 2023). Evolutionary rescue that requires two successive mutations has been investigated using diffusion approximation by Martin et al. (2013).

Methods

Evolutionary model

We follow the number of cancer cells that have one of three different genotypes at time t: wildtype, w_t; aneuploid, a_t; and mutant, m_t. These cells divide and die with rates λ_k and μ_k (for $k = w, a, m$). The difference between the division and death rate is $\Delta_k = \lambda_k - \mu_k$. We assume the population of cells is under a strong stress, such as drug therapy, to which the wildtype genotype is susceptible or sensitive and therefore $\Delta_w < 0$, whereas the mutant is resistant to the stress, $\Delta_m > 0$. We analyze three scenarios: in the first, aneuploid cells are partially resistant, $\Delta_m > \Delta_a > 0$; in the second, aneuploid cells are tolerant, $0 > \Delta_a > \Delta_w$ (see Brauner et al., 2016, for the distinction between susceptible, resistant, and tolerant); in the third, aneuploid cells are non-growing, stationary or "barely growing", that is, either slightly tolerant or slightly resistant, such that $\Delta_a \approx 0$. We assume that both chromosomal missegregation and mutation occur during the process of mitosis. Wildtype cells may divide and then missegregate to become aneuploids at rate $u\lambda_w$. Both aneuploid and wildtype cells may divide and mutate to become mutants at rates $v\lambda_a$ and $v\lambda_w$, respectively, which we assume is lower than the division rates, $v \cdot \max{(\lambda_w, \lambda_a)} < \min{(\lambda_w, \lambda_a, \lambda_m)}$. See Figure 1 for a schematic representation of the model and Figure 2 for sample trajectories of the different genotypes for $u = 0\,(\mathbf{A}), \Delta_a \ll 0\,(\mathbf{B}), \Delta_a \approx 0\,(\mathbf{C}), \Delta_a \gg 0\,(\mathbf{D})$.

Stochastic simulations

Simulations are performed using a *Gillespie algorithm* (Gillespie, 1976, 1977) implemented in Python (Van Rossum and Others, 2007). The simulation monitors the number of cells of each type: wildtype, aneuploid, and mutant. The wildtype population initially consists of $w_0 = N$ cells, whereas the other cell types are initially absent.

The state of the stochastic system at time t is represented by the triplet (w_t, a_t, m_t). The following describes the events that may occur (right column), the rates at which they occur (middle column), and the effect these events have on the state (left column, see Figure 1):

$$
\begin{aligned}
(+1, 0, 0): &\quad \lambda_w w_t (1 - u - v) \quad \text{(birth of wildtype cell)}, \\
(-1, 0, 0): &\quad \mu_w w_t \quad \text{(death of wildtype cell)}, \\
(0, +1, 0): &\quad u\lambda_w w_t \quad \text{(wildtype cell divides and becomes aneuploid)}, \\
(0, 0, +1): &\quad v\lambda_w w_t \quad \text{(wildtype cell divides and becomes mutant)}, \\
(0, +1, 0): &\quad \lambda_a a_t (1 - v) \quad \text{(birth of aneuploid cell)}, \\
(0, -1, 0): &\quad \mu_a a_t \quad \text{(death of aneuploid cell)}, \\
(0, 0, +1): &\quad v\lambda_a a_t \quad \text{(aneuploid cell divides and becomes mutant)}, \\
(0, 0, +1): &\quad \lambda_m m_t \quad \text{(birth of mutant cell)}, \\
(0, 0, -1): &\quad \mu_m m_t \quad \text{(death of mutant cell)}.
\end{aligned}
$$

For the remaining of this paper we assume that the division rates for wildtype and aneuploid cells can be written as $\lambda_w w_t (1 - u - v) \approx \lambda_w w_t$ and $\lambda_a a_t (1 - v) \approx \lambda_a a_t$ because $u, v \ll 1$ (see Table 1). Each iteration of the simulation loop starts with computing the rates v_j of each event j. We then draw the time until the next event, Δt, from an exponential distribution whose rate parameter is the sum of the rates of all events, such that $\Delta t \sim Exp(\sum_j v_j)$. Then, we randomly determine which event occurred, where the probability for event j is $p_j = v_j / \sum_i v_i$. Finally, we update the number of cells of each type according to the event that occurred and update the time from t to $t + \Delta t$. We repeat these iterations until either the population becomes extinct (the number of cells of all types is zero) or the number of

mutant cells is high enough so that its extinction probability is $< 0.1\%$, that is until

$$m_t > \left\lfloor \frac{3\log 10}{\log\left(\lambda_m/\mu_m\right)} \right\rfloor + 1.$$

τ**-leaping.** When simulations are slow (e.g. due to large population size), we utilize τ-leaping (Gillespie, 2001), where change in number of cells of genotype i in a fixed time interval Δt is Poisson distributed with mean $v_i\Delta t$. If the change in number of cells is negative and larger then the subpopulation size then the subpopulation size is updated to be zero.

Density-dependent growth. In our analysis we assume that lineages produced by cells from the initial population divide and die independently of each other, which may be unrealistic, as cells usually compete for resources. A more realistic model includes competition for limited resources and spatial structure, which may play an important role in the development of cancer (e.g., Martens et al., 2011). To simulate birth and death rates that depend on the number of cells in the population, we transform the rates of division and death to the following:

$$\lambda'_w = \lambda_w,$$
$$\mu'_w = \mu_w,$$
$$\lambda'_a = \lambda_a,$$
$$\mu'_a = \mu_a + \lambda_a \frac{w+a+m}{K},$$
$$\lambda'_m = \lambda_m,$$
$$\mu'_m = \mu_m + \lambda_m \frac{w+a+m}{K}.$$

where K is the maximum carrying capacity. The effective carrying capacity of this model is $K_e = K\Delta_a/\lambda_a \approx 10^6$ for $K = 10^8, \lambda_a = 0.0901, \mu_a = 0.09$.

Code and data availability.

All source code is available online at https://github.com/yoavram-lab/EvolutionaryRescue.

Results

Evolutionary rescue probability

In our model, *evolutionary rescue* occurs when resistant cells appear and fixate ($m_t \gg 1$) in the population before the population becomes extinct ($w_t = a_t = m_t = 0$). Aneuploidy may contribute to evolutionary rescue by either preventing (when $\Delta_a > 0$) or delaying (when $0 > \Delta_a > \Delta_w$) the extinction of the population before mutant cells appear and fixate. We assume independence between clonal lineages starting from an initial population of N wildtype cells (we check the effect of density-dependent growth on our results below). We therefore define p_w as the probability that a lineage starting from a single wildtype cell avoids extinction by acquiring drug resistance. Thus, $N^* = 1/p_w$ is the threshold tumor size above which evolutionary rescue is very likely, and the rescue probability is given by

$$p_{\text{rescue}} = 1 - \left(1 - p_w\right)^N \approx 1 - e^{-Np_w} = 1 - e^{-N/N^*}. \tag{2}$$

where the approximation $(1 - p_w) \approx e^{-p_w}$ assumes that p_w (but not necessarily Np_w) is small. Indeed, when $N < 1/p_w$, then the probability for evolutionary rescue is $p_{\text{rescue}} \approx Np_w$ and when $N > 1/p_w$,

it is $p_{\text{rescue}} \approx 1$, justifying the definition of N^* as the threshold tumor size.

In the Appendix, we use the theory of multi-type branching processes to find approximate expressions eqs. (10), (13) and (17) for p_w in different regimes. Substituting these into $N^* = 1/p_w$, we find approximations for the threshold tumor size, N^*. For these approximations, an important quantity is $T^* = (4v\lambda_a^2\Delta_m/\lambda_m)^{-1/2}$, which is the critical time an aneuploid lineage needs to survive to produce a resistant mutant that avoids random extinction. First, if aneuploidy is very rare ($u\lambda_a T^* < 1$), or if aneuploidy is rare ($u\lambda_a < -\Delta_a$) and very sensitive to the drug ($\Delta_a T^* < -1$), then rescue will likely occur by a direct resistance mutation in a sensitive cell, such that

$$N_m^* \approx \frac{|\Delta_w|}{v\lambda_w} \cdot \frac{\lambda_m}{\Delta_m}. \tag{3}$$

Here, $|\Delta_w|/(v\lambda_w)$ is the ratio of the rate at which wild-type cells are decreasing in number and the rate at which they are mutating.

Otherwise, aneuploidy is frequent enough ($u\lambda_a > \max(-\Delta_a, 1/T^*)$) to affect the evolution of drug resistance. The threshold tumor size, N^*, can then be approximated by one of the following cases, depending on $\Delta_a T^*$, the change in the log of the aneuploid population size during the critical time,

$$N_a^* \approx \frac{|\Delta_w|}{u\lambda_w} \cdot \begin{cases} \frac{|\Delta_a|}{v\lambda_a} \cdot \frac{\lambda_m}{\Delta_m}, & \Delta_a T^* \ll -1 \text{ (partially tolerant aneuploids)}, \\ 2\lambda_a T^*, & -1 \ll \Delta_a T^* \ll 1 \text{ (stationary aneuploids)}, \\ \frac{\lambda_a}{\Delta_a}, & \Delta_a T^* \gg 1 \text{ (resistant aneuploids)}. \end{cases} \tag{4}$$

The first line describes the case in which aneuploids are still effectively killed by the treatment, but not as quickly as the wild type. In the second case, the aneuploids are sufficiently resistant that the size of each aneuploid lineage is expected to remain roughly constant. In both of these first two cases, aneuploidy increases the probability of rescue by slowing or halting the decrease of the cancer population, allowing more opportunities for producing resistant mutants. In the third case, aneuploidy provides sufficient resistance for the aneuploid population to re-grow the tumor even without additional resistance mutations. Note that in this case there is no dependence on the parameters characterizing mutants or their production (v, λ_m, and Δ_m). Comparing these approximations to results of stochastic evolutionary simulations, we find that the approximations perform very well (Figures 3 and 4). Increasing the the missegregation rate u and aneuploid growth rate Δ_a reduces the threshold tumor size and facilitates the evolution of drug resistance (Figure 4).

Using eqs. (3) and (4), we can find the ratio of threshold tumor size for rescue via aneuploidy (u is high) or via direct mutation (u is low),

$$\frac{N_a^*}{N_m^*} \approx \begin{cases} \frac{|\Delta_a|}{u\lambda_a}, & \Delta_a T^* \ll -1, \\ \frac{1}{u}\left(v \cdot \frac{\Delta_m}{\lambda_m}\right)^{1/2}, & -1 \ll \Delta_a T^* \ll 1, \\ v\frac{\Delta_m}{\lambda_m} \cdot \left(u\frac{\Delta_a}{\lambda_a}\right)^{-1}, & \Delta_a T^* \gg 1. \end{cases} \tag{5}$$

In all cases, the effect of aneuploidy increases (i.e., the threshold size ratio decreases) when the aneuploidy rate u increases (Figure 4B). Increasing the aneuploid growth rate Δ_a also leads to an increased role of aneuploidy, although the effect is minor when $|\Delta_a|$ is small compared to T^* (Figure 4A). Increasing the mutation rate v decreases the effect of aneuploidy and increases the probability of evolutionary rescue.

In the first case, $|\Delta_a|/(u\lambda_a)$ is the ratio of the expected time for an aneuploid lineage to appear, $1/(u\lambda_a)$, and the expected time until that lineage disappears, $1/|\Delta_a|$. In the third case, $\left(v\frac{\Delta_m}{\lambda_m}\right)/\left(u\frac{\Delta_a}{\lambda_a}\right)$ is the ratio of the rates of formation of resistant mutants that avoid extinction and partially resistant

aneuploids that avoid extinction. In the second case, $\frac{1}{u}\left(v \cdot \frac{\Delta_m}{\lambda_m}\right)^{1/2} = \sqrt{\frac{\Delta_a}{u\lambda_a} \cdot v\frac{\Delta_m}{\lambda_m} \cdot \left(u\frac{\Delta_a}{\lambda_a}\right)^{-1}}$, which is the geometric mean of the first and third cases.

Interestingly, increasing both the aneuploid division rate, λ_a, and the aneuploid death rate, μ_a, such that the growth rate Δ_a remains constant, leads to decreases in T^*, and therefore to the second case. In this case, increasing the division rate λ_a should also increase the mutation rate $v\lambda_a$ in aneuploid cells, as mutations mostly occur during division, so overall the threshold tumor size N_a^* is unaffected by the division rate λ_a (i.e., $d\lambda_a T^*/d\lambda_a = 0$). Thus, if aneuploids rapidly die due to the drug but compensate by rapidly dividing, further increasing the division rate will *not* facilitate adaptation. For the parameter values of $\lambda_w = 0.1, \lambda_a = 0.0899, \lambda_m = 0.1, \mu_w = 0.14, \mu_a = 0.09, \mu_m = 0.09, u = 10^{-2}, v = 10^{-7}$ we are in the partially resistant aneuploid case and obtain the ratio $N_a^*/N_m^* \approx |\Delta_a|/u\lambda_a = 0.11$ which means that the presence of aneuploidy reduces the threshold population by approximately 90%. We observe that aneuploidy has a significant contribution towards the tumor overcoming chemotherapeutic drugs.

Density-dependent growth. In our analysis we used branching processes, which assume that growth (division and death) is density-independent. However, growth may be limited by resources (oxygen, nutrients, etc.) and therefore depend on cell density. We therefore performed stochastic simulations of a logistic growth model with carrying capacity K (see Methods). We find that our approximations agree with results of simulations with density-dependent growth for biologically relevant parameter values (Figure 7).

Standing vs. de-novo genetic variation. In the above we assumed that at the onset of drug treatment, the initial tumor consisted entirely of wildtype cells that are drug sensitive. However, aneuploid cells are likely generated even before onset of treatment at some rate $\tilde{u} \leq u$ (because the treatment itself may promote generation of aneuploid cells (Mason et al., 2017, Wang et al., 2019)), which are likely to have a deleterious effect in the absence of the drug, s (Giam and Rancati, 2015, Replogle et al., 2020). But if the number of cells in the tumor N is large (as expected if the tumor is to be treated with a drug), there may already be a fraction $f \approx \tilde{u}\lambda_w/s$ (we assume that the division rate of the wildtype in a drug-free environment is equal to the division rate of the wildtype in the environment affected by the anti-cancer drug) of aneuploid cells in the population.

Therefore, the threshold tumor size with standing generation variation, $\tilde{N}_a^*$, is similar to the ratio with de-novo variation, N_a^*, except that the sensitive growth rate $|\Delta_w|$ is replaced with the aneuploidy cost, s, such that

$$\frac{\tilde{N}_a^*}{N_a^*} = \frac{u}{\tilde{u}} \frac{s}{|\Delta_w|}. \tag{6}$$

Therefore, standing genetic variation will drive adaptation to the drug if Δ_w is very negative due to a stronger effect of the drug on sensitive cells, or if s is very small due to a low cost of aneuploidy in the pre-drug conditions. In contrast, de-novo aneuploids will have a stronger effect on adaptation if the aneuploidy cost s is large, the effect of the drug is weak (Δ_w is small), or if the drug induces the appearance of aneuploid cells ($u > \tilde{u}$). Comparing these approximations to results of stochastic evolutionary simulations, we find that the approximations perform very well (Figure 5). We derive s by using the formula $s = \tilde{u}\lambda_w/f$ and obtaining the fraction of aneuploid cancer cells f from (Lukow et al., 2021) who mixed together wildtype and aneuploid cell at $50 : 50$ ratio, cultured them in drug-free environment and observed the ratio evolve as a function of time.

For the parameter values of $\lambda_w = 0.1, \mu_w = 0.14, u = 10^{-2}, \tilde{u} = 10^{-3}, s = 5 \cdot 10^{-4}$ the ratio of the threshold population sizes is $\tilde{N}_a^*/N_a^* \approx 0.125$ which means that standing genetic variation is the main driver of adaptation even when a relatively small fraction cancer cells are aneuploid in the drug-free environment (in this case $f = 20\%$). Furthermore, most tumors display significantly higher levels of aneuploidy such that $f \approx 95\%$ even before cancer treatment. In this case, the population threshold

6

ratio becomes $\tilde{N}_a^*/N_a^* \approx 0.0025$ and standing genetic variation is a very significant driver of adaptation to the chemotherapeutic drug.

Recurrence time due to evolutionary rescue

Even when evolutionary rescue occurs and leads to recurrence of the tumor, it may take a long time. When the expected number of resistant lineages that avoid extinction is small the overall expected recurrence time can be estimated by adding two terms: the mean waiting time for evolutionary rescue– the appearance of a resistant lineage that avoid extinction– (which we denote the mean evolutionary rescue time) and the expected time for proliferation of that lineage back to the original tumor size, N (which we denote the mean proliferation time). However, when the expected number of resistant lineages is large the population of mutant cells behaves deterministically and the mean recurrence time cannot be separated into the mean evolutionary rescue time and mean proliferation time.

Evolutionary rescue time. In Appendix C we derive an approximation for τ_1, the expected rescue time without aneuploidy ($u = 0$), and τ_2, the expected rescue time with aneuploidy ($u > 0$). Figure 10 shows the agreement between these approximations and simulation results for intermediate and large tumor sizes.

Recurrence time. In Appendix D we approximate the mean time for the population of mutant cancer cells to reach the initial population size N which we denote as the recurrence time. Figure 8 shows the agreement between our approximations and simulations. For values of N smaller then 10^8 the mean recurrence time can be approximated as the sum of the mean time for the first rescue muation to appear and the mean time for the lineage generated by that mutation to reach size N. For $N > 10^8$ the behavior of the mutant cancer cell population is deterministic and the mean proliferation time becomes constant.

Distribution of evolutionary rescue time – with and without aneuploidy. In Appendix E we derive the probability that by time t a successful mutant has been generated. Figure 6 show the agreement between our formula and simulation results for the case when aneuploidy is present and when it is absent. We observe that aneuploidy start to have an effect on adaptation for timescales greater then 100 days.

Distribution of recurrence time. In Appendix F we derive the probability that mutant cancer cell population reaches N at time t. Figure 9 shows agreement between our approximations and stochastic simulations for various values of N.

Discussion

We have modeled a tumor–a population of cancer cells–exposed to drug treatment that causes the population to decline in size towards potential extinction. In this scenario, the tumor can be "evolutionary rescued", or escape extinction, via two paths. In the direct path, a sensitive cell acquires a mutation that confers resistance that allows it to rapidly grow. In the indirect path, a sensitive cell first becomes aneuploid, which diminishes the effect of the drug, and then an aneuploid cell acquires a mutation that confers resistance (Figure 1).

Using multitype branching processes, we derived the probability of evolutionary rescue of the population of cancer cells under different scenarios for the effect of aneuploidy, ranging from tolerance to partial resistance. We obtained exact and approximate expressions for the probability of evolutionary

rescue (eq. (2)). Our results show that the probability of evolutionary rescue increases with the initial tumor size N, the sensitive growth rate Δ_w, the mutation rate v, and the aneuploidy rate u.

Evolutionary rescue   When aneuploid cells are partially resistant to the drug ($\Delta_w \ll 0 \ll \Delta_a \ll \Delta_m$), evolutionary rescue can be approximated by a one-step process in which aneuploidy itself rescues the population (Figure 4A). When aneuploidy only provides tolerance to the drug ($\Delta_w \ll \Delta_a \ll 0 \ll \Delta_m$), it cannot rescue the population. Instead, it acts as a *stepping stone* through which the resistant mutant can appear more rapidly, given that the aneuploid cell population declines slower then the sensitive cell population (Figure 2). In this case, aneuploidy provides two benefits. First, it delays the extinction of the population–providing more time for appearance of the resistance mutation. Second, it increases the population size relative to a sensitive population–providing more cells in which mutations can occur, i.e., it increases the mutation supply, $Nuv\lambda_w\lambda_a/|\Delta_w\Delta_a|$.

We find that aneuploidy can have a significant effect on evolutionary rescue (Figure 3). Interestingly, aneuploidy is unlikely to contribute to evolutionary rescue in primary tumors in which the number of cells is large enough ($N > 10^8$) for the appearance of resistant mutation directly in sensitive cells before these cells become extinct (Figure 3). However, aneuploidy can have a crucial role in evolutionary rescue of secondary tumors, in which the number of sensitive cells may be below the detection threshold of $\sim 10^7$ (Bozic et al., 2013). This can have an impact on the recurrence of cancer after the resection of the primary tumor through secondary tumors which are too small to be detected and for which chemotherapy is employed to prevent cancer relapse and are estimated to cause the majority of cancer-related deaths (Chaffer and Weinberg, 2011).

Given the fact that the mean time for such secondary tumors to overcome chemotherapy can be of the order of 1000 days (Figure 10A), this can explain the reappearance of cancer even after initial remission. The theoretical predictions for the mean rescue time for tumors smaller then 10^8 is greater then 4 years which is consistent with previous estimates of the recurrence time of tumors after resection (Avanzini and Antal, 2019).

Paradoxically, we observe from Figure 10 that the mean time of a rescue mutation to appear is significatly shorter for the case when $u = 0$ when compared to the case $u > 0$, however this can be explained by the fact this mean time is conditioned on evolutionary rescue and, as a result, aneuploidy increase the *window of opportunity* in which a rescue mutation could appear thus increasing the mean time as well (Figure 2).

We hypothesized that presence of *standing variation* –the existence of a subpopulation of aneuploid cancer cells before therapy begins–can facilitate evolutionary rescue by reducing the waiting time for the appearance of aneuploid cells. Indeed, we observe that even when a small fraction of the initial tumor is aneuploid, evolutionary rescue is more likely to occur through this existing standing variation, rather then through *de novo* aneuploid cells (Figure 5).

We observe from Figure 9 that the probability of the mutant cell population reaching size N is approximately zero before time τ_2^r which is the recurrence time for the deterministic case. This can be explained as follows: in the deterministic case there is a sufficient number of lineages produced such that there exists a lineage where each descendant will only reproduce and not die; the time it takes for this lineage to reach N is the lower bound for the time of all other lineages to reach N and this time cannot be smaller then τ_2^r by definition. Given that for small values of N we expect that at most a single lineage will rescue the tumor, this lineage cannot reach N before τ_2^r for the deterministic case eq. (28).

Experimental future direction   Our model's predictions may be tested by experiments (Martin et al., 2013). For example, to study the effects of initial tumor size on the probability of evolutionary rescue, a large culture mass can be propagated from a single cancer cell in permissive conditions and then diluted to a range of starting tumor sizes. Afterwards, these tumors may be exposed to anti-cancer drugs that induces aneuploidy or to saline solution for control (Ippolito et al., 2021). Cell density can

then be measured by optical density and a population exposed to the drug is considered extinct if the optical density is lower when compared to the control case. We compare to the predictions of our model to see if the tumors with initial size bellow the threshold (4) are more likely to go extinct.

Directions of future research Even though our model has been designed for cancer it can be extended to understand to understand evolutionary in different biological contexts, for example, how yeast subject to stress can overcome extinction with the help of aneuploidy (Pompei and Cosentino Lagomarsino, 2023). Additionally, the heterogeneity of aneuploidy is a fact the we did not account for, as not all the aneuploidy lineages generated have the same growth rate Δ_a. This can be corrected by fixing the aneuploidy death rates and sampling the aneuploidy growth rates from a distribution $f(\Delta_a|\mu_a)$ Martin et al. (2013). Furthermore, tumor heterogeneity is also a factor for pre-existing genetic variation where the fitness of the aneuploid cells can be drawn from a distribution upon which selection acts when the tumor is exposed to a strong stress.

We have assumed that cancer cell lineages are independent of each other. However, this may not be the case, as cancer cells compete for resources (e.g., blood supply). Nevertheless, we find that when the effective carrying capacity is not too large ($K \sim 10^8, K_e \sim 10^6$) our approximation for the probability of evolutionary rescue agrees with results of stochastic simulations with density-dependent growth (Figure 7). Future work may focus on scenarios with small carrying capacity by analyzing density-dependent branching processes (Harris, 1963, Klebaner, 1997).

Conclusions Our paper analyzed the role that aneuploidy plays in tumor adaptation to the effects of anti-cancer drugs. Our study quantitatively confirms that aneuploidy plays an important role in tumors overcoming exposure to chemotherapeutic drugs when the tumor size is small or intermediate. Very large tumors can escape anti-cancer drugs through direct mutation while smaller ones are able to obtain the beneficial mutation through an aneuploid intermediary (Figure 3). As a result, therapies which increase the rate of aneuploidy in tumors in order to combat cancer might have an adverse effect on patient outcomes.

Acknowledgements

References

Allen, L. J. (2010), *An introduction to stochastic processes with applications to biology*, CRC press.

Avanzini, S. and Antal, T. (2019), 'Cancer recurrence times from a branching process model', *PLoS computational biology* **15**(11), e1007423.

Bakker, B., Schubert, M., Bolhaqueiro, A. C., Kops, G. J., Spierings, D. C. and Foijer, F. (2023), 'Predicting CIN rates from single-cell whole genome sequencing data using an *in silico* model', *bioRxiv* pp. 2023–02.

Ben-David, U. and Amon, A. (2020), 'Context is everything: aneuploidy in cancer', *Nature Reviews Genetics* **21**(1), 44–62.

Bozic, I., Reiter, J. G., Allen, B., Antal, T., Chatterjee, K., Shah, P., Moon, Y. S., Yaqubie, A., Kelly, N., Le, D. T. et al. (2013), 'Evolutionary dynamics of cancer in response to targeted combination therapy', *eLife* **2**, e00747.

Brauner, A., Fridman, O., Gefen, O. and Balaban, N. Q. (2016), 'Distinguishing between resistance, tolerance and persistence to antibiotic treatment', *Nature Reviews Microbiology* **14**(5), 320–330.

Carja, O. and Plotkin, J. B. (2017), 'The evolutionary advantage of heritable phenotypic heterogeneity', *Scientific reports* **7**(1), 1–12.

Carja, O. and Plotkin, J. B. (2019), 'Evolutionary rescue through partly heritable phenotypic variability', *Genetics* **211**(3), 977–988.

Carlson, J. A. (2003), 'Tumor doubling time of cutaneous melanoma and its metastasis', *The American journal of dermatopathology* **25**(4), 291–299.

Chaffer, C. L. and Weinberg, R. A. (2011), 'A perspective on cancer cell metastasis', *science* **331**(6024), 1559–1564.

Christine, J. Y., Regan, S., Liu, G., Alemara, S. and Heng, H. H. (2018), 'Understanding aneuploidy in cancer through the lens of system inheritance, fuzzy inheritance and emergence of new genome systems', *Molecular cytogenetics* **11**(1), 1–13.

Cobbold, C. A. and Stana, R. (2020), 'Should I stay or should I go: partially sedentary populations can outperform fully dispersing populations in response to climate-induced range shifts', *Bulletin of Mathematical Biology* **82**(2), 1–21.

Del Monte, U. (2009), 'Does the cell number 10^9 still really fit one gram of tumor tissue?', *Cell cycle* **8**(3), 505–506.

Giam, M. and Rancati, G. (2015), 'Aneuploidy and chromosomal instability in cancer: a jackpot to chaos', *Cell division* **10**(1), 1–12.

Gillespie, D. T. (1976), 'A general method for numerically simulating the stochastic time evolution of coupled chemical reactions', *Journal of computational physics* **22**(4), 403–434.

Gillespie, D. T. (1977), 'Exact stochastic simulation of coupled chemical reactions', *The journal of physical chemistry* **81**(25), 2340–2361.

Gillespie, D. T. (2001), 'Approximate accelerated stochastic simulation of chemically reacting systems', *The Journal of chemical physics* **115**(4), 1716–1733.

Harris, T. E. (1963), *The theory of branching processes*, Vol. 6, Springer Berlin.

Harsch, M. A., Zhou, Y., HilleRisLambers, J. and Kot, M. (2014), 'Keeping pace with climate change: stage-structured moving-habitat models', *The American Naturalist* **184**(1), 25–37.

Ippolito, M. R., Martis, V., Martin, S., Tijhuis, A. E., Hong, C., Wardenaar, R., Dumont, M., Zerbib, J., Spierings, D. C., Fachinetti, D. et al. (2021), 'Gene copy-number changes and chromosomal instability induced by aneuploidy confer resistance to chemotherapy', *Developmental cell* **56**(17), 2440–2454.

Klebaner, F. (1997), Population and density dependent branching processes, *in* 'Classical and modern branching processes', Springer, pp. 165–169.

Komarova, N. L., Sadovsky, A. V. and Wan, F. Y. (2008), 'Selective pressures for and against genetic instability in cancer: a time-dependent problem', *Journal of The Royal Society Interface* **5**(18), 105–121.

Komarova, N. L., Sengupta, A. and Nowak, M. A. (2003), 'Mutation–selection networks of cancer initiation: tumor suppressor genes and chromosomal instability', *Journal of theoretical biology* **223**(4), 433–450.

Komarova, N. L. and Wodarz, D. (2004), 'The optimal rate of chromosome loss for the inactivation of tumor suppressor genes in cancer', *Proceedings of the National Academy of Sciences* **101**(18), 7017–7021.

Levien, E., Min, J., Kondev, J. and Amir, A. (2021), 'Non-genetic variability in microbial populations: survival strategy or nuisance?', *Reports on Progress in Physics* **84**(11), 116601.

Loeb, L. A. (2001), 'A mutator phenotype in cancer', *Cancer research* **61**(8), 3230–3239.

Lukow, D. A., Sausville, E. L., Suri, P., Chunduri, N. K., Wieland, A., Leu, J., Smith, J. C., Girish, V., Kumar, A. A., Kendall, J. et al. (2021), 'Chromosomal instability accelerates the evolution of resistance to anti-cancer therapies', *Developmental cell* **56**(17), 2427–2439.

Marrec, L. and Bank, C. (2023), 'Evolutionary rescue in a fluctuating environment: periodic versus quasi-periodic environmental changes', *Proceedings of the Royal Society B* **290**(1999), 20230770.

Marrec, L. and Bitbol, A.-F. (2020), 'Adapt or perish: Evolutionary rescue in a gradually deteriorating environment', *Genetics* **216**(2), 573–583.

Martens, E. A., Kostadinov, R., Maley, C. C. and Hallatschek, O. (2011), 'Spatial structure increases the waiting time for cancer', *New journal of physics* **13**(11), 115014.

Martin, G., Aguilée, R., Ramsayer, J., Kaltz, O. and Ronce, O. (2013), 'The probability of evolutionary rescue: towards a quantitative comparison between theory and evolution experiments', *Philosophical Transactions of the Royal Society B: Biological Sciences* **368**(1610), 20120088.

Martin, G., Elena, S. F. and Lenormand, T. (2007), 'Distributions of epistasis in microbes fit predictions from a fitness landscape model', *Nature genetics* **39**(4), 555–560.

Mason, J. M., Wei, X., Fletcher, G. C., Kiarash, R., Brokx, R., Hodgson, R., Beletskaya, I., Bray, M. R. and Mak, T. W. (2017), 'Functional characterization of cfi-402257, a potent and selective mps1/ttk kinase inhibitor, for the treatment of cancer', *Proceedings of the National Academy of Sciences* **114**(12), 3127–3132.

Michor, F., Iwasa, Y., Vogelstein, B., Lengauer, C. and Nowak, M. A. (2005), Can chromosomal instability initiate tumorigenesis?, *in* 'Seminars in cancer biology', Vol. 15, Elsevier, pp. 43–49.

Nowak, M. A., Komarova, N. L., Sengupta, A., Jallepalli, P. V., Shih, I.-M., Vogelstein, B. and Lengauer, C. (2002), 'The role of chromosomal instability in tumor initiation', *Proceedings of the National Academy of Sciences* **99**(25), 16226–16231.

Orr, H. A. and Unckless, R. L. (2014), 'The population genetics of evolutionary rescue', *PLoS genetics* **10**(8), e1004551.

Osmond, M. M., Otto, S. P. and Martin, G. (2020), 'Genetic paths to evolutionary rescue and the distribution of fitness effects along them', *Genetics* **214**(2), 493–510.

Pavelka, N., Rancati, G. and Li, R. (2010), 'Dr Jekyll and Mr Hyde: role of aneuploidy in cellular adaptation and cancer', *Current opinion in cell biology* **22**(6), 809–815.

Pompei, S. and Cosentino Lagomarsino, M. (2023), 'A fitness trade-off explains the early fate of yeast aneuploids with chromosome gains', *Proceedings of the National Academy of Sciences* **120**(15), e2211687120.

Replogle, J. M., Zhou, W., Amaro, A. E., McFarland, J. M., Villalobos-Ortiz, M., Ryan, J., Letai, A., Yilmaz, O., Sheltzer, J., Lippard, S. J. et al. (2020), 'Aneuploidy increases resistance to chemotherapeutics by antagonizing cell division', *Proceedings of the National Academy of Sciences* **117**(48), 30566–30576.

Rew, D. and Wilson, G. (2000), 'Cell production rates in human tissues and tumours and their significance. part ii: clinical data', *European Journal of Surgical Oncology (EJSO)* **26**(4), 405–417.

Rutledge, S. D., Douglas, T. A., Nicholson, J. M., Vila-Casadesús, M., Kantzler, C. L., Wangsa, D., Barroso-Vilares, M., Kale, S. D., Logarinho, E. and Cimini, D. (2016), 'Selective advantage of trisomic human cells cultured in non-standard conditions', *Scientific reports* **6**(1), 22828.

Schukken, K. M. and Foijer, F. (2018), 'CIN and aneuploidy: different concepts, different consequences', *Bioessays* **40**(1), 1700147.

Tanaka, M. M. and Wahl, L. M. (2022), 'Surviving environmental change: when increasing population size can increase extinction risk', *Proceedings of the Royal Society B* **289**(1976), 20220439.

Uecker, H. and Hermisson, J. (2011), 'On the fixation process of a beneficial mutation in a variable environment', *Genetics* **188**(4), 915–930.

Uecker, H. and Hermisson, J. (2016), 'The role of recombination in evolutionary rescue', *Genetics* **202**(2), 721–732.

Uecker, H., Otto, S. P. and Hermisson, J. (2014), 'Evolutionary rescue in structured populations', *The American Naturalist* **183**(1), E17–E35.

Uecker, H., Setter, D. and Hermisson, J. (2015), 'Adaptive gene introgression after secondary contact', *Journal of mathematical biology* **70**, 1523–1580.

Van Rossum, G. and Others (2007), Python programming language, *in* 'USENIX Annu. Tech. Conf.'.

Wahl, L. and Campos, P. R. (2023), 'Evolutionary rescue on genotypic fitness landscapes', *Journal of the Royal Society Interface* **20**(208), 20230424.

Wang, S., Zhang, M., Liang, D., Sun, W., Zhang, C., Jiang, M., Liu, J., Li, J., Li, C., Yang, X. et al. (2019), 'Molecular design and anticancer activities of small-molecule monopolar spindle 1 inhibitors: A medicinal chemistry perspective', *European Journal of Medicinal Chemistry* **175**, 247–268.

Weissman, D. B., Desai, M. M., Fisher, D. S. and Feldman, M. W. (2009), 'The rate at which asexual populations cross fitness valleys', *Theoretical population biology* **75**(4), 286–300.

Weissman, D. B., Feldman, M. W. and Fisher, D. S. (2010), 'The rate of fitness-valley crossing in sexual populations', *Genetics* **186**(4), 1389–1410.

Wilson, B. A., Pennings, P. S. and Petrov, D. A. (2017), 'Soft selective sweeps in evolutionary rescue', *Genetics* **205**(4), 1573–1586.

Zhou, Y. (2022), 'Range shifts under constant-speed and accelerated climate warming', *Bulletin of Mathematical Biology* **84**(1), 1.

Zhu, J., Tsai, H.-J., Gordon, M. R. and Li, R. (2018), 'Cellular stress associated with aneuploidy', *Developmental cell* **44**(4), 420–431.
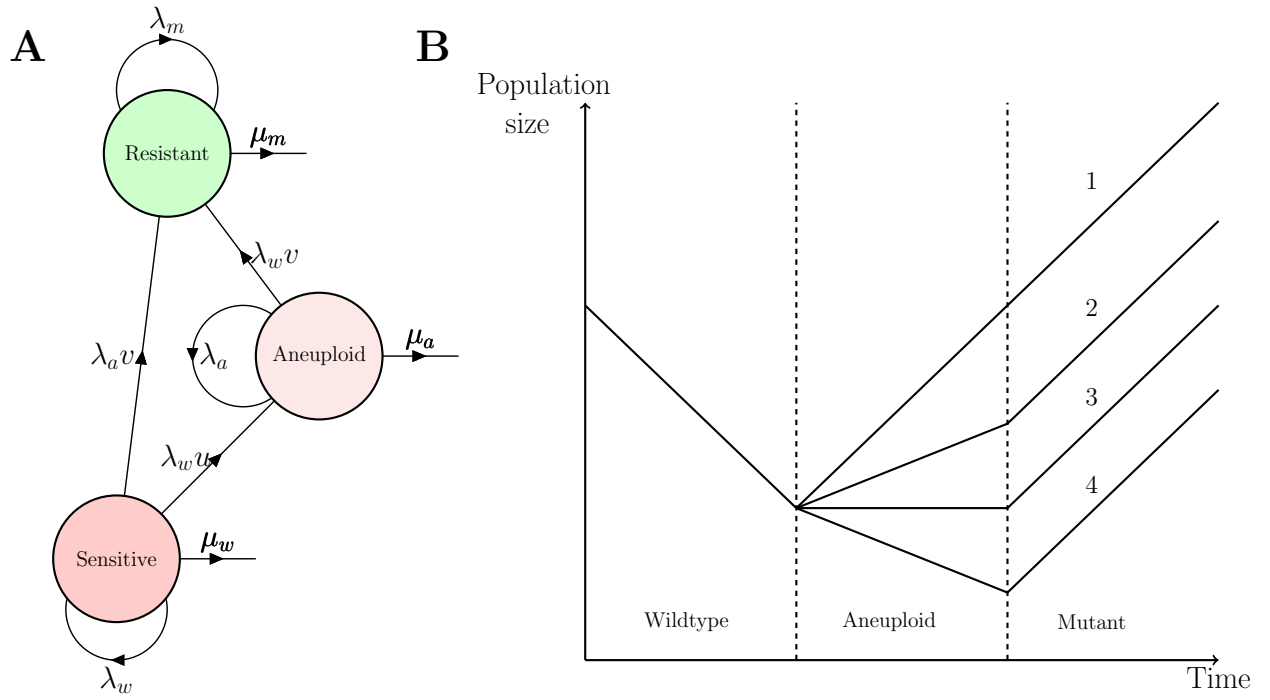
Figure 1: Model illustration. **(A)** A population of cancer cells is composed of wildtype, aneuploid, and mutant cells, which divide with rates λ_w, λ_a, and λ_m and die at rates μ_w, μ_a, and μ_m, respectively. Wildtype cells can divide and become aneuploid at rate $u\lambda_w$. Both aneuploid and wildtype cells can divide and acquire a beneficial mutation with rate $v\lambda_a$ and $v\lambda_w$, respectively. Color denotes the relative growth rates of the three genotypes such that $\lambda_w - \mu_w < \lambda_a - \mu_a < \lambda_m - \mu_m$. **(B)** The wildtype and the mutant are susceptible and resistant, respectively, to the drug. The aneuploid may be tolerant (4), stationary (3), partially resistant (2) or fully resistant (1).

	Name	Value	Units	References
N	Initial tumor size	$10^7 - 10^9$	cells	Del Monte (2009)
λ_w	Wildtype division rate	0.1	1/days	Bozic et al. (2013), Rew and Wilson (2000)
μ_w	Wildtype death rate	$0.11 - 0.17$	1/days	Bozic et al. (2013)
λ_a	Aneuploid division rate*	$0.06 - 0.1$	1/days	-
μ_a	Aneuploid death rate*	0.09	1/days	-
λ_m	Mutant division rate	0.1	1/days	Bozic et al. (2013), Rew and Wilson (2000)
μ_m	Mutant death rate	0.09	1/days	Bozic et al. (2013), Carlson (2003)
u	Missegregation rate	$10^{-3} - 10^{-2}$	1/cell division	Bakker et al. (2023)
v	Mutation rate	$10^{-7} - 10^{-5}$	1/gene/cell division	Loeb (2001)
$\tilde{u}$	Missegregation rate in the drug free environment*	10^{-3}	1/cell division	-
s	Selection coefficient of aneuploidy in the drug free environment	$0.3 \cdot 10^{-3} - 10^{-3}$	1/days	Lukow et al. (2021)

Table 1: Model parameters. The * symbol in the Name column means that for those parameters the values have not been selected from a paper. Aneuploid death rate μ_a is set to the same value as the mutant death rates, μ_m, given that aneuploidy increases resistance to chemotherapeutics, such as cisplatin, by antagonizing cell division (Replogle et al., 2020). Aneuploid birth rate λ_a is set such that the aneuploid growth rate $\Delta_w \ll \Delta_a \ll \Delta_m$. For the missegregation rate in the drug free environment $\tilde{u}$ we choose the lower-end value of u as the chemotherapeutic drugs we want to model increase the rate of aneuploidy (Mason et al., 2017, Wang et al., 2019). We note that we have modified the parameters from Bozic et al. (2013) by starting their analysis from the fact that wildtype/mutant birth rate is $\lambda_{w,m} = \log 2/T \approx 0.1$ instead of their value of 0.14 where T is the doubling time in the absence of cellular death obtained from Rew and Wilson (2000). We suspect the value of 0.1 was obtained as $1/T$ because T can also be defined as the average time between cell divisions in the absence of cell death Avanzini and Antal (2019). We derive the fitness cost s by using the formula $s = \tilde{u}\lambda_w/f$ and obtaining the fraction of aneuploid cancer cells f from (Lukow et al., 2021) who mixed together wildtype and aneuploid cell at 50 : 50 ratio, cultured them in drug-free environment and observed the ratio evolve as a function of time.
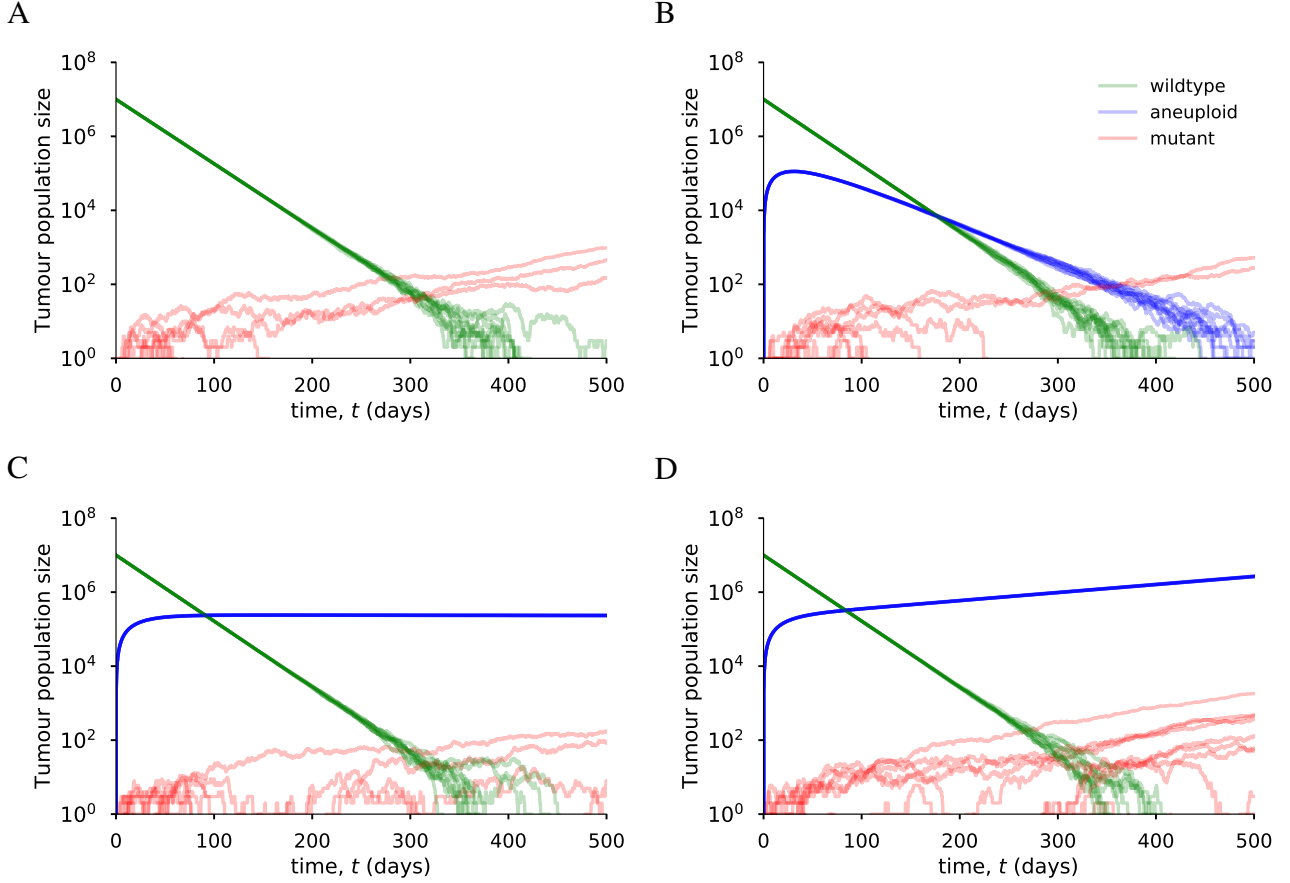
Figure 2: Sample trajectories of the different genotypes as a function of time. **(A)** Whe the missegregation rate $u = 0$ evolutionary rescue is only possible through direct mutation and in most cases the tumour will be cured by the drug. **(B)** When the aneuploidy growth rate $\Delta_a \ll 0$ we observe similar dynamic to case **(A)** as direct mutation is the only viable route toward evolutionary rescue for the tumor. **(C)** Intermediate aneuploid growth rates $\Delta_a \approx 0$ generates the appearence of aneuploid lineages even after the wildtype population has gone extinct thus increasing the chance of evolutionary rescue. **(D)** As the growth rate of the aneuploid becomes positive we observe that the tumour is rescued by the aneuploid cancer cell population. Each plot features 10 trajectories of (w_t, a_t, m_t) as a function of time t for the following parameter values: $\lambda_w = 0.1, \lambda_m = 0.1, \mu_w = 0.14, \mu_a = 0.09, \mu_m = 0.09, v = 10^{-7}, N = 10^7$. For **(A)** we set $u = 0$, for **(B)** $\lambda_a = 0.065, u = 10^{-2}$, for **(C)** $\lambda_a = 0.0899, u = 10^{-2}$ and for **(D)** $\lambda_a = 0.095, u = 10^{-2}$.

16
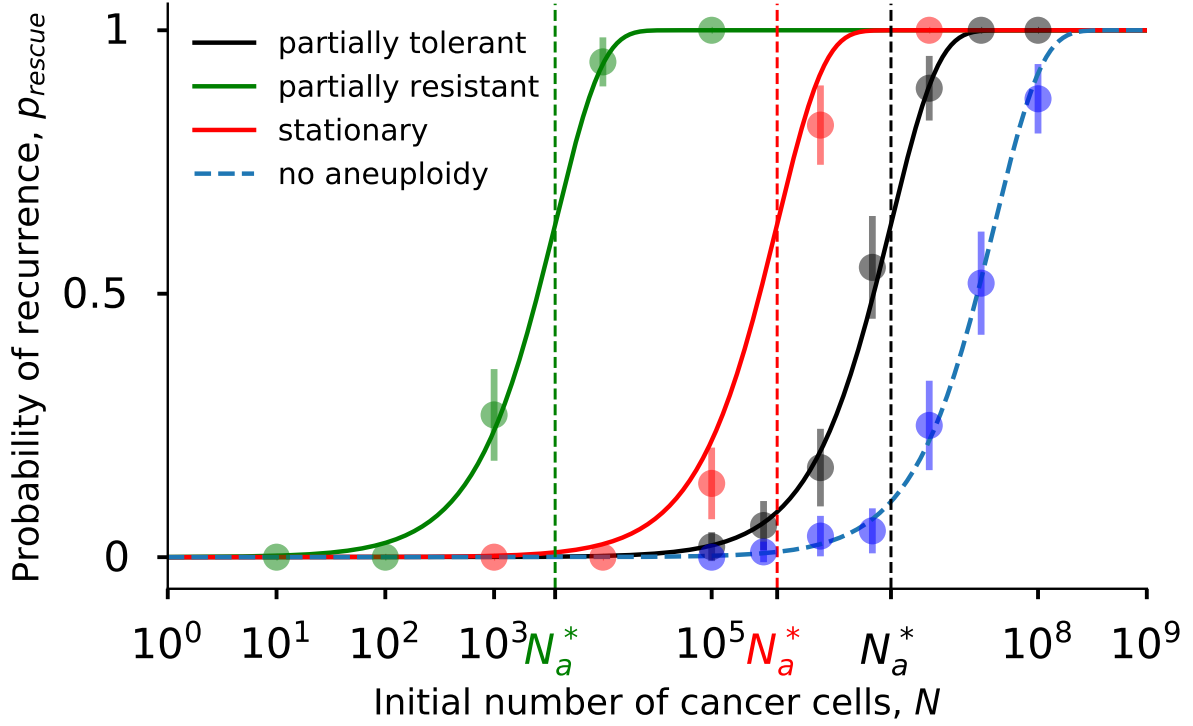
Figure 3: Aneuploidy facilitates evolutionary rescue of cancer under drug treatment. The probability of evolutionary rescue (i.e. the probability that the population does not go to extinction), p_{rescue}, as a function of the initial tumor size, N. Dashed vertical line shows the threshold tumor size, N_a^*, above which the probability is very high. Blue dashed line represents the probability of evolutionary rescue as a function of N without aneuploidy ($u = 0$). The black line represents the case with tolerant aneuploidy ($u = 10^{-2}, \lambda_a = 0.0899$), the red line represents the case with stationary aneuploidy ($u = 10^{-2}, \lambda_a = 0.08999$) and the green line represents the case with partially resistant aneuploidy ($u = 10^{-2}, \lambda_a = 0.095$). The dots represent numerical simulations and the error bars represent 95% confidence interval of the form $p \pm 1.96\sqrt{p(1-p)/n}$ where p is the probability of that the tumor has adapted to the stress and $n = 100$ is the number of simulations. Parameters: $\lambda_w = 0.1, \lambda_m = 0.1, \mu_w = 0.14, \mu_a = 0.09, \mu_m = 0.09, v = 10^{-7}$.
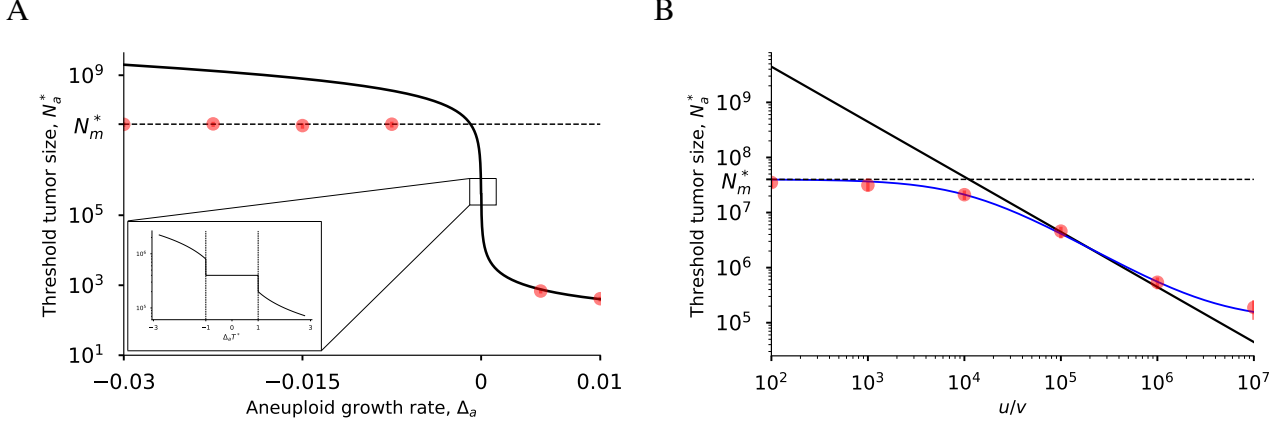
Figure 4: Aneuploidy growth rate and missegregation rate impact the evolutionary rescue of cancer under drug treatment. (A) The threshold tumor size N_a^* as a function of the aneuploid growth rate Δ_a. The dashed horizontal line shows N_m^*, the threshold tumor size without aneuploidy ($u = 0$). The red dots represent numerical simulations. The inset highlights the case when aneuploidy cancer cells are non-growing. When aneuploid growth rate is close to or higher than zero, aneuploidy decreases the threshold tumor size, thereby facilitating evolutionary rescue. Parameters: $\lambda_w = 0.1, \lambda_m = 0.1, \mu_w = 0.14, \mu_a = 0.09, \mu_m = 0.09, u = 10^{-2}, v = 10^{-7}$. (B) The threshold tumor size N_a^* as a function of the ratio of aneuploidy and mutation rates, u/v. The dashed horizontal line shows N_m^*, the threshold tumor size without aneuploidy ($u = 0$). The blue line represents the exact formula for threshold tumor size N_a^* while the solid black line represents the approximation eq. (4). The red dots represent numerical simulations. When the aneuploidy rate is much higher than the mutation rate, aneuploidy decreases the threshold tumor size, thereby facilitating evolutionary rescue. Parameters: $\lambda_w = 0.1, \lambda_m = 0.0899, \lambda_m = 0.1, \mu_w = 0.14, \mu_a = 0.09, \mu_m = 0.09, v = 10^{-7}$. For the threshold tumor sizes the error bars represent the 95% confidence interval obtained through bootstrapping in the following steps: **(1)** we simulate p_{rescue} 100 times; **(2)** we sample with replacement which we store in S; **(4)** for each element of this sample we obtain $N_a^* = 1/p_w$ using $p_w = -1/N_s \log\left(1 - \bar{S}\right)$ where $\bar{S}$ is the mean of S and N_s is an arbitrary value of the initial population size we selected in order to calculate p_{rescue}; **(5)** we repeat steps **(2)**-**(4)** 100 times to obtain N_a^* and we select the upper and lower limits such that 95% of the values of N_a^* lie in the interval given by the bounds.
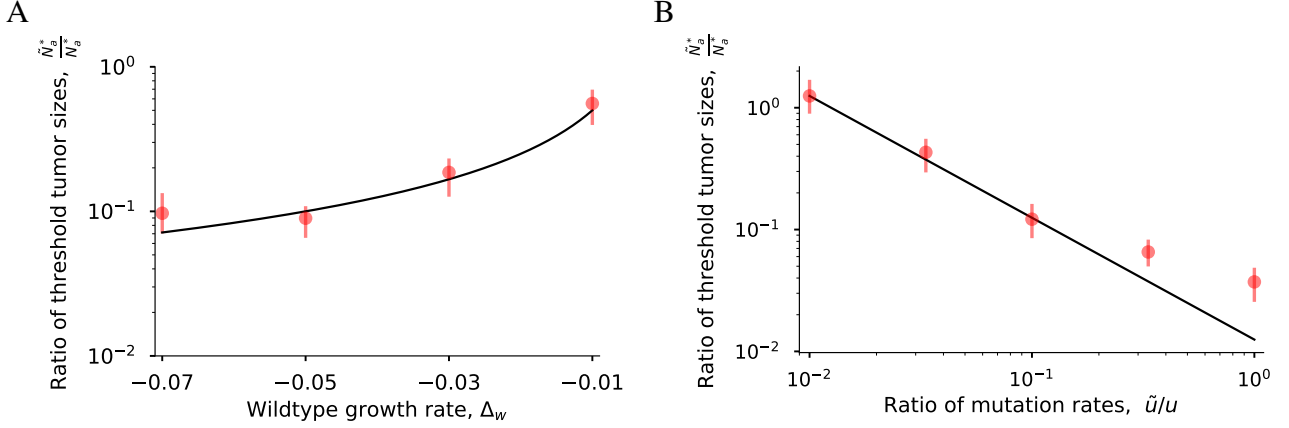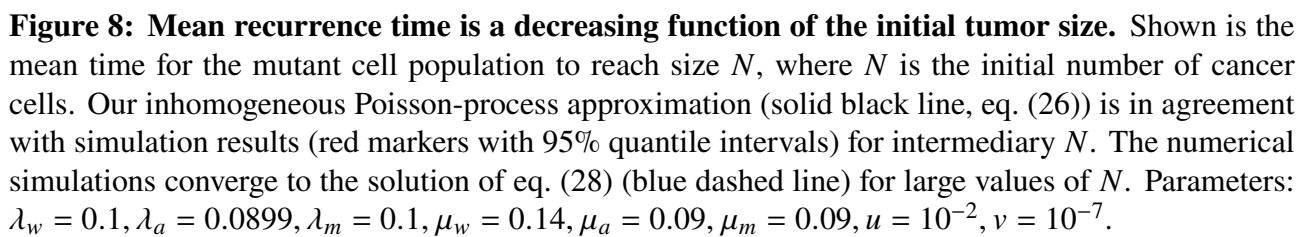
Figure 5: Standing genetic variation facilitates evolutionary rescue of cancer under drug treatment. **(A)** The ratio of threshold tumor size $\tilde{N}_a^*$ when a fraction $\frac{\tilde{u}\lambda_w}{s}$ is aneuploid at the start of treatment and N_a^* as a function of the wildtype growth rate Δ_w. The red dots represents numerical simulations and the error bars represent the 95% confidence intervals obtained with bootstrapping explained below. Standing genetic variation will drive adaptation to the drug if Δ_w is very negative due to a stronger effect of the drug on sensitive cells. Parameters: $\lambda_w = 0.1, \lambda_a = 0.0899, \lambda_m = 0.1, \mu_a = 0.09, \mu_m = 0.09, \tilde{u} = 10^{-3}, u = 10^{-2}, v = 10^{-7}$. **(B)** The ratio of threshold tumor size $\tilde{N}_a^*$ when a fraction $\frac{\tilde{u}\lambda_w}{s}$ is aneuploid at the start of treatment and N_a^* as a function of the the ratio of aneuploidy rates $\tilde{u}/u$. The red dots represents numerical simulations and the error bars represent the 95% confidence intervals obtained with bootstrapping explained below. De-novo aneuploids will have larger contribution to the appearance of drug resistance if the drug induces the appearance of aneuploid cells ($u \gg \tilde{u}$). Parameters: $\lambda_w = 0.1, \lambda_a = 0.0899, \lambda_m = 0.1, \mu_w = 0.14, \mu_a = 0.09, \mu_m = 0.09, \tilde{u} = 10^{-3}, v = 10^{-7}$. For the ratio of the threshold tumor sizes the error bars represent the 95% confidence interval obtained through bootstrapping in the following steps: **(1)** we simulate p_{rescue} 100 times for both the case when $f = \tilde{u}\lambda_w/s$ and $f = 0$; **(2)** we sample with replacement which we store in S_0 and S_f; **(4)** for each element of S_0 we obtain $N_a^* = 1/p_w$ using $p_w = -1/N_s \log\left(1 - \bar{S}\right)$ where $\bar{S}$ is the mean of S_0 and N_s is an arbitrary value of the initial population size we selected in order to calculate p_{rescue}; **(5)** for each element of S_f we obtain $\tilde{N}_a^* = 1/p_a$ using $p_a = -f/N_s \log\left(1 - \bar{S}\right)$ where $\bar{S}_f$ is the mean of S_f and N_s is an arbitrary value of the initial population size we selected in order to calculate p_{rescue}; **(6)** we repeat steps **(2)**-**(5)** 100 times to obtain $\tilde{N}_a^*/N_a^*$ and we select the upper and lower limits such that 95% of the values of $\tilde{N}_a^*/N_a^*$ lie in the interval given by the bounds.
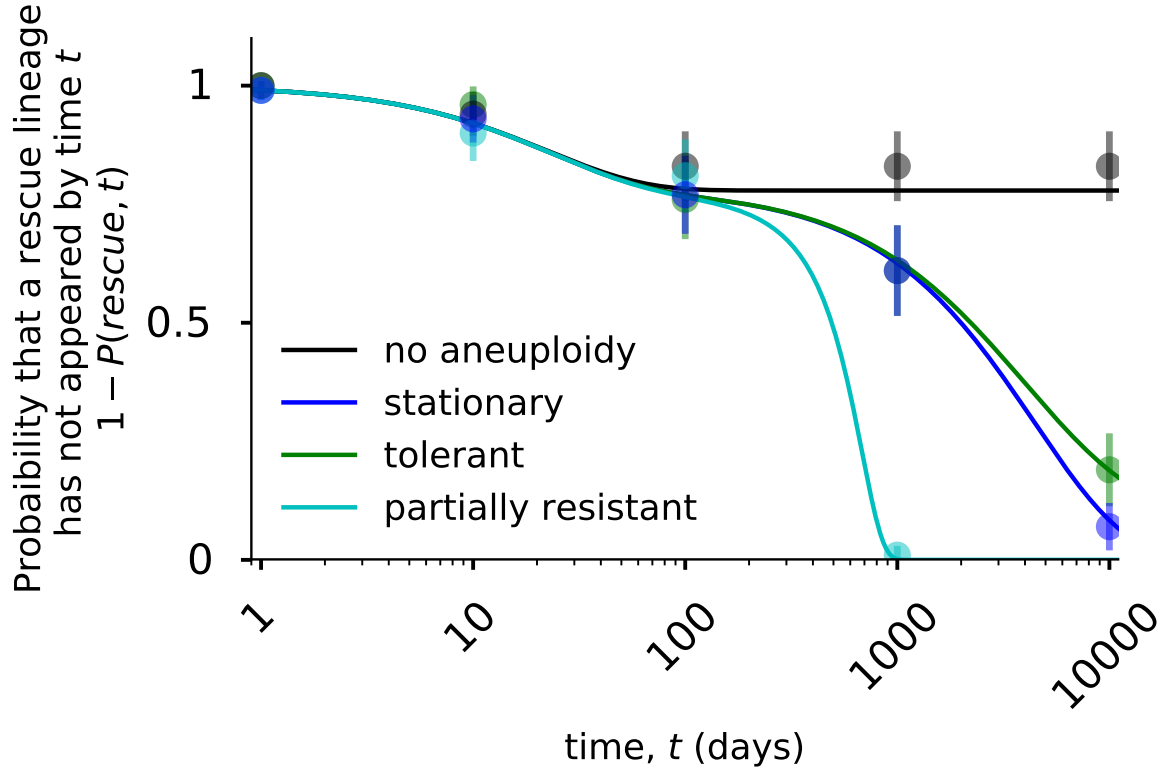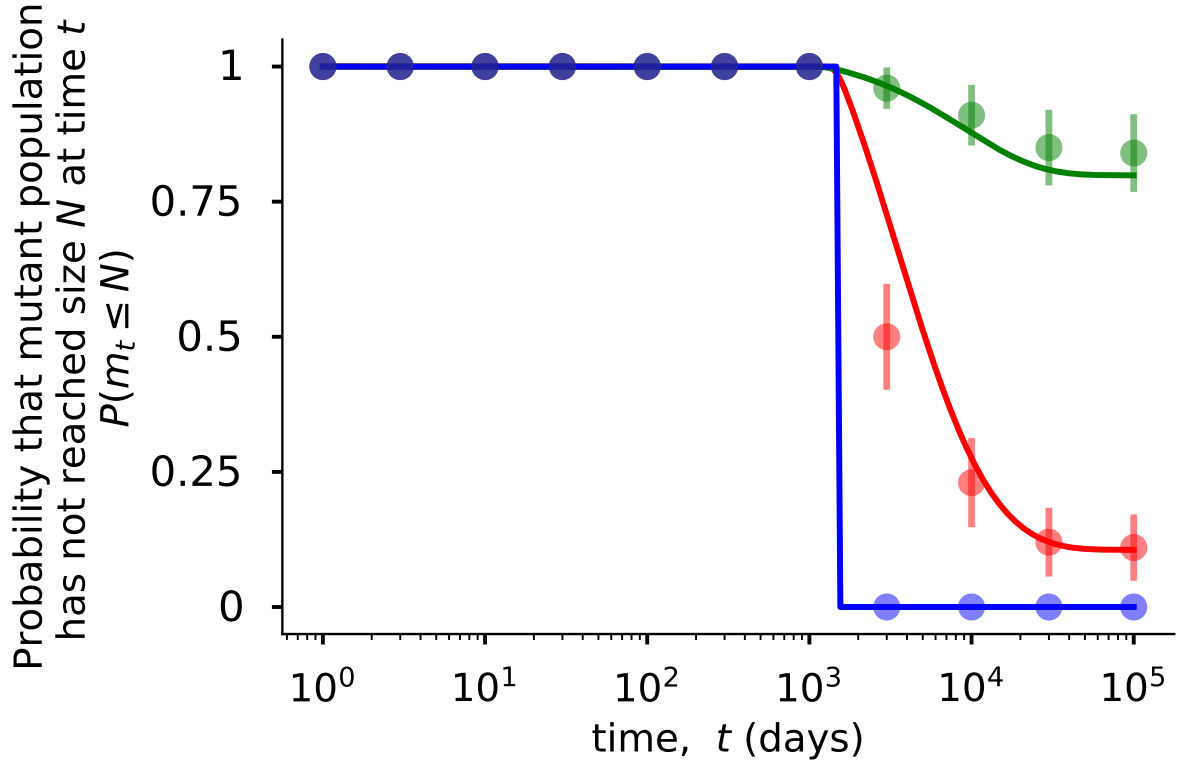
Figure 6: Aneuploidy is a key diver of cancer adaptation. Plot of the probability that a successful mutant has not appeared by time t. The green line represents the case with tolerant aneuploidy ($u > 0, \lambda_a = 0.0899$), the blue line represents the case with non-growing aneuploidy ($u > 0, \lambda_a = 0.089999$), the cyan line represents the case with partially resistant aneuploidy ($u > 0, \lambda_a = 0.095$) and the black line represents the case without aneuploidy ($u = 0$). The dots represent numerical simulations. For the simulations we have chosen the following parameters: $\lambda_w = 0.1, \lambda_m = 0.1, \mu_w = 0.14, \mu_a = 0.09, \mu_m = 0.09, u = 10^{-2}, v = 10^{-7}, N = 10^7$. The error bars represent 95% confidence interval of the form $p \pm 1.96\sqrt{p(1-p)/n}$ where p is the probability of that a successful mutant has not been generated and $n = 100$ is the number of simulations. As time increases, aneuploidy plays an important role in helping the cancer cell population escape extinction.
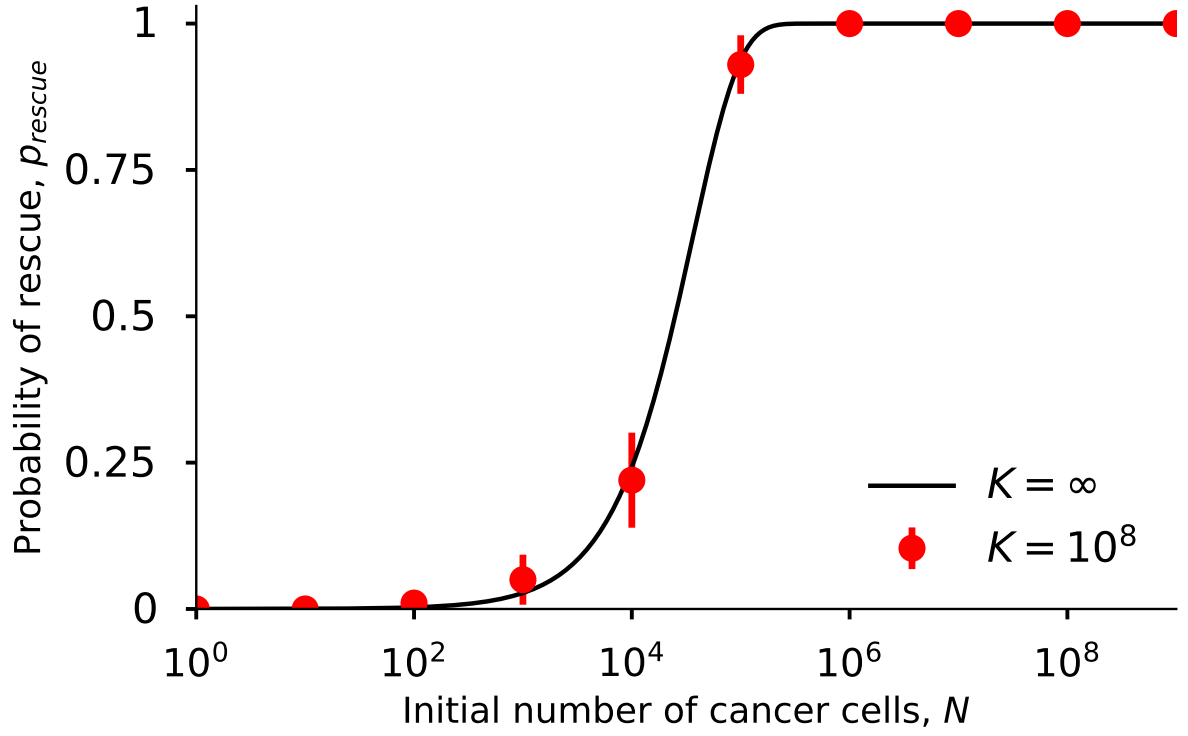
Figure 7: Density dependent growth does not affect the accuracy of our model. Comparison of results of simulations with density-dependent growth (red markers with with 95% CI) and the approximation formula (black line, eq. (4) in eq. (2)) with maximum carrying capacity $K = 10^8$ and effective carrying capacity $K_e = K\Delta_a/\lambda_a \approx 10^6$. The error bars represent 95% confidence interval of the form $p \pm 1.96\sqrt{p(1-p)/n}$ where p is the probability that the tumor has adapted to the stress and $n = 100$ is the number of simulations. Parameters: $\lambda_w = 0.1, \lambda_a = 0.0901, \lambda_m = 0.1, \mu_w = 0.14, \mu_a = 0.09, \mu_m = 0.09, u = 10^{-2}, v = 10^{-7}, K = 10^8$.

Figure 8: Mean recurrence time is a decreasing function of the initial tumor size. Shown is the mean time for the mutant cell population to reach size N, where N is the initial number of cancer cells. Our inhomogeneous Poisson-process approximation (solid black line, eq. (26)) is in agreement with simulation results (red markers with 95% quantile intervals) for intermediary N. The numerical simulations converge to the solution of eq. (28) (blue dashed line) for large values of N. Parameters: $\lambda_w = 0.1, \lambda_a = 0.0899, \lambda_m = 0.1, \mu_w = 0.14, \mu_a = 0.09, \mu_m = 0.09, u = 10^{-2}, v = 10^{-7}$.

Figure 9: Plot of the probability that a mutant cancer cell population has not reached size N at time t. The green line represents the case where $N = 10^6$, the red line represents $N = 10^7$ and the blue line represents the case where $N = 10^{10}$. Increasing the initial tumor size guarantees that the tumor recurrence. The markers represent stochastic simulations and the error bars represents 95% confidence interval of the form $p \pm 1.96\sqrt{p(1-p)/n}$ where p is the probability of that a mutant population size has not reached N and $n = 100$ is the number of simulations. Parameters: $\lambda_w = 0.1, \lambda_a = 0.0899, \lambda_m = 0.1, \mu_w = 0.14, \mu_a = 0.09, \mu_m = 0.09, u = 10^{-2}, v = 10^{-7}$.

Appendices

Appendix A: Survival probability of a single lineage

To analyze evolutionary rescue in this model, we use the framework of *multitype branching processes* (Harris, 1963, Weissman et al., 2009). This allows us to find explicit expressions for the *survival probability*: the probability that a lineage descended from a single cell does not become extinct.

Let p_w, p_a, and p_m be the survival probabilities of a population consisting initially of single wildtype cell, aneuploid cell, or mutant cell, respectively. The complements $1 - p_w$, $1 - p_a$, and $1 - p_m$ are the extinction probabilities, which satisfy each its respective equation (Harris, 1963),

$$
\begin{aligned}
1 - p_w =& \frac{\mu_w}{\lambda_w + \mu_w + u\lambda_w + v\lambda_w} + \frac{u\lambda_w}{\lambda_w + \mu_w + u\lambda_w + v\lambda_w} (1 - p_a)(1 - p_w) + \\
& \frac{\lambda_w}{\lambda_w + \mu_w + u\lambda_w + v\lambda_w}(1 - p_w)^2 + \frac{v\lambda_w}{\lambda_w + \mu_w + u\lambda_w + v\lambda_w}(1 - p_m)(1 - p_w), \\
1 - p_a =& \frac{\mu_a}{\lambda_a + \mu_a + v\lambda_a} + \frac{v\lambda_a}{\lambda_a + \mu_a + v\lambda_a}(1 - p_m)(1 - p_a) + \frac{\lambda_a}{\lambda_a + \mu_a + v\lambda_a}(1 - p_a)^2, \\
1 - p_m =& \frac{\mu_m}{\lambda_m + \mu_m} + \frac{\lambda_m}{\lambda_m + \mu_m}(1 - p_m)^2.
\end{aligned}
\tag{7}
$$

The survival probabilities are given by the smallest solution for each quadratic equation (Uecker et al., 2015). Therefore we have

$$
\begin{aligned}
p_w &= \frac{\lambda_w - \mu_w - u\lambda_w p_a - v\lambda_w p_m + \sqrt{(\lambda_w - \mu_w - u\lambda_w p_a - v\lambda_w p_m)^2 + 4\lambda_w^2(up_a + vp_m)}}{2\lambda_w}, \\
p_a &= \frac{\lambda_a - \mu_a - v\lambda_a p_m + \sqrt{(\lambda_a - \mu_a - v\lambda_a p_m)^2 + 4\lambda_a^2 vp_m}}{2\lambda_a}, \\
p_m &= \frac{\lambda_m - \mu_m}{\lambda_m}.
\end{aligned}
\tag{8}
$$

Note that the equation for p_w depends on both p_a and p_m, and the equation for p_a depends on p_m. To proceed, we can plug the solution for p_m and p_a into the solution for p_w. We perform this for three different scenarios.

Scenario 1: Aneuploid cells are partially resistant

We first assume that aneuploidy provides partial resistance to drug therapy, $\lambda_a > \mu_a$, and that this resistance is significant, $(\lambda_a - \mu_a - v\lambda_a p_m)^2 > 4\lambda_a^2 vp_m$. We thus rewrite eq. (8) as

$$
\begin{aligned}
p_w &= \frac{\lambda_w - \mu_w - u\lambda_w p_a - v\lambda_w p_m}{2\lambda_w}\left(1 - \sqrt{1 + \frac{4\lambda_w^2(vp_m + up_a)}{(\lambda_w - \mu_w - u\lambda_w p_a - v\lambda_w p_m)^2}}\right), \text{ and} \\
p_a &= \frac{\lambda_a - \mu_a - v\lambda_a p_m}{2\lambda_a}\left(1 + \sqrt{1 + \frac{4\lambda_a^2 vp_m}{(\lambda_a - \mu_a - v\lambda_a p_m)^2}}\right).
\end{aligned}
$$

Using the quadratic Taylor expansion $\sqrt{1 + x} = 1 + x/2 + O(x^2)$ and assuming $u, v \ll 1$, we obtain the following approximation for the survival probability of a population initially consisting of a single

wildtype cell,

$$p_w \approx -\frac{v\lambda_w p_m + u\lambda_w p_a}{\lambda_w - \mu_w - u\lambda_w p_a - v\lambda_w p_m} \tag{9}$$

$$\approx -\frac{1}{\lambda_w - \mu_w}\left[\frac{u\lambda_w(\lambda_a - \mu_a)}{\lambda_a} + \frac{uv\lambda_w\lambda_a(\lambda_m - \mu_m)}{\lambda_m(\lambda_a - \mu_a)} + \frac{v\lambda_w(\lambda_m - \mu_m)}{\lambda_m}\right].$$

Now uv is very small, and if we use the fact that $v \ll u$, we have:

$$p_w \approx \frac{u\lambda_w}{|\Delta_w|} \cdot \frac{\Delta_a}{\lambda_a}. \tag{10}$$

However, if aneuploidy is very rare such that

$$\frac{u\lambda_w\Delta_a}{\lambda_a} < \frac{v\lambda_w\Delta_m}{\lambda_m} \Rightarrow u\lambda_a < \frac{v\lambda_a^2\Delta_m}{\lambda_m} \cdot \frac{1}{\Delta_a} < \frac{v\lambda_a^2\Delta_m}{\lambda_m} \cdot \frac{1}{\sqrt{4\lambda_a^2 v p_m}} \Rightarrow u\lambda_a < T^*,$$

where $T^* = (4v\lambda_a^2\Delta_m/\lambda_m)^{-1/2}$ and in the second inequality we used the fact that $\Delta_a^2 > 4\lambda_a^2 v p_m$. In this case adaptation is through direct mutation and:

$$p_w \approx \frac{v\lambda_w}{|\Delta_w|} \cdot \frac{\Delta_m}{\lambda_m}.$$

Scenario 2: Aneuploid cells are tolerant.

We now assume that aneuploidy provides tolerance to drug therapy, that is, the number of aneuploid cells significantly declines over time, but at a lower rate than the number of wildtype cells, $\lambda_w - \mu_w < \lambda_a - \mu_a < 0$. We also assume that the decline are significant, $(\lambda_a - \mu_a - v\lambda_a p_m)^2 > 4\lambda_a^2 v p_m$. We rewrite eq. (8) as

$$p_w = \frac{\lambda_w - \mu_w - u\lambda_w p_a - v\lambda_w p_m}{2\lambda_w}\left(1 - \sqrt{1 + \frac{4\lambda_w^2(v p_m + u p_a)}{(\lambda_w - \mu_w - u\lambda_w p_a - v\lambda_w p_m)^2}}\right),$$

$$p_a = \frac{\lambda_a - \mu_a - v\lambda_a p_m}{2\lambda_a}\left(1 - \sqrt{1 + \frac{4\lambda_a^2 v p_m}{(\lambda_a - \mu_a - v\lambda_a p_m)^2}}\right). \tag{11}$$

Since $u, v \ll 1$, the term in the root can be approximated using a 1st-order Taylor expansion. So, substituting the expressions for p_a and p_m, we have

$$p_w \approx -\frac{v\lambda_w p_m + u\lambda_w p_a}{\lambda_w - \mu_w - u\lambda_w p_a - v\lambda_w p_m}$$

$$\approx \frac{1}{\lambda_w - \mu_w - u\lambda_w p_a - v\lambda_w p_m}\left[\frac{uv\lambda_w\lambda_a(\lambda_m - \mu_m)}{\lambda_m(\lambda_a - \mu_a - v\lambda_a)} - \frac{v\lambda_w(\lambda_m - \mu_m)}{\lambda_m}\right]$$

$$\approx \frac{v\lambda_w(\lambda_m - \mu_m)}{\lambda_m(\lambda_w - \mu_w)}\left[\frac{u\lambda_a}{(\lambda_a - \mu_a)} - 1\right] \tag{12}$$

$$= \frac{v\lambda_w\Delta_m}{\lambda_m|\Delta_w|}\left(\frac{u\lambda_a}{|\Delta_a|} + 1\right).$$

If we assume that $u\lambda_a > |\Delta_a|$ then we have:

$$p_w \approx \frac{u\lambda_w}{|\Delta_w|} \cdot \frac{v\lambda_a}{|\Delta_a|} \cdot \frac{\Delta_m}{\lambda_m}. \tag{13}$$

Scenario 3: Aneuploid cells are stationary

We now assume that the growth rate of aneuploid cells is close to zero (either positive or negative), such that $\left(\Delta_a - v\lambda_a p_m\right)^2 \ll 4\lambda_a^2 v p_m$. We rewrite eq. (8) as

$$p_a = \frac{\lambda_a - \mu_a - v\lambda_a p_m + 2\sqrt{\lambda_a^2 v p_m}\left(1 + \frac{\left(\lambda_a - \mu_a - v\lambda_a p_m\right)^2}{4\lambda_a^2 v p_m}\right)^{\frac{1}{2}}}{2\lambda_a}. \tag{14}$$

Using a following Taylor series expansion for small $\left(\lambda_a - \mu_a - v\lambda_a p_m\right)^2 / 4\lambda_a^2 v p_m$,

$$\left(1 + \frac{\left(\lambda_a - \mu_a - v\lambda_a p_m\right)^2}{4\lambda_a^2 v p_m}\right)^{\frac{1}{2}} = 1 + \frac{\left(\lambda_a - \mu_a - v\lambda_a p_m\right)^2}{8\lambda_a^2 v p_m} + \cdots,$$

we obtain the approximation

$$
\begin{aligned}
p_a &\approx \frac{\lambda_a - \mu_a - v\lambda_a p_m + 2\sqrt{\lambda_a^2 v p_m}\left[1 + \frac{\left(\lambda_a - \mu_a - v\lambda_a p_m\right)^2}{8\lambda_a^2 v p_m}\right]}{2\lambda_a} \\
&= \frac{\lambda_a - \mu_a - v\lambda_a p_m + 2\sqrt{\lambda_a^2 v p_m} + \frac{\left(\lambda_a - \mu_a - v\lambda_a p_m\right)^2}{4\sqrt{\lambda_a^2 v p_m}}}{2\lambda_a} \\
&= \frac{\left(\lambda_a - \mu_a - v\lambda_a p_m + 2\sqrt{\lambda_a^2 v p_m}\right)^2 + 4\lambda_a^2 v p_m}{8\lambda_a \sqrt{\lambda_a^2 v p_m}} \\
&= \frac{4\lambda_a^2 v p_m + 4\lambda_a^2 v p_m \left(1 + \frac{\lambda_a - \mu_a - v\lambda_a p_m}{2\sqrt{\lambda_a^2 v p_m}}\right)^2}{8\lambda_a \sqrt{\lambda_a^2 v p_m}} \\
&= \frac{1}{2\lambda_a}\left(\lambda_a - \mu_a - v\lambda_a p_m + 2\sqrt{\lambda_a^2 v p_m}\right).
\end{aligned} \tag{15}
$$

Plugging this in eq. (9), the survival probability of a population starting from one wildtype individual is

$$
\begin{aligned}
p_w &\approx -\frac{1}{\lambda_w - \mu_w - u\lambda_w p_a - v\lambda_w p_m}\left[v\lambda_w \frac{\lambda_m - \mu_m}{\lambda_m} + \frac{u\lambda_w}{2\lambda_a}\left(\lambda_a - \mu_a - v\lambda_a p_m + 2\sqrt{\lambda_a^2 v p_m}\right)\right] \\
&= -\frac{1}{\lambda_w - \mu_w - u\lambda_w - v\lambda_w}\left[v\lambda_w \frac{\lambda_m - \mu_m}{\lambda_m} + \frac{u\lambda_w}{2\lambda_a}\left(\lambda_a - \mu_a - v\lambda_a p_m\right) + u\lambda_w\sqrt{\frac{v\left(\lambda_m - \mu_m\right)}{\lambda_m}}\right] \\
&\approx -\frac{1}{\Delta_w}\left[v\lambda_w \frac{\Delta_m}{\lambda_m} + \frac{u\lambda_w\left(\Delta_a - v\lambda_a\right)}{2\lambda_a} + u\lambda_w\sqrt{\frac{v\Delta_m}{\lambda_m}}\right].
\end{aligned} \tag{16}
$$

Using the fact that

$$\left(\Delta_a - v\lambda_a p_m\right)^2 \ll 4\lambda_a^2 v p_m \implies \frac{\Delta_a - v\lambda_a p_m}{2\lambda_a} \ll \sqrt{\frac{v\lambda_a\Delta_m}{\lambda_m}},$$

and $v \ll u$ we obtain:

$$p_w \approx \frac{u\lambda_w}{|\Delta_w|} \cdot \sqrt{\frac{v\lambda_a\Delta_m}{\lambda_m}}. \tag{17}$$

Appendix B: Evolutionary rescue probability

Using the fact that $\Delta_a - v\lambda_a p_m \approx \Delta_a$ we write the condition $(\Delta_a - v\lambda_a p_m)^2 \ll 4\lambda_a^2 v p_m$ as:

$$\Delta_a^2 \ll 4\lambda_a^2 v p_m \Rightarrow -1 \ll \Delta_a T^* \ll 1,$$

where $T^* = (4v\lambda_a^2 \Delta_m/\lambda_m)^{-1/2}$. Substituting eqs. (10), (13) and (17) into eq. (2), the evolutionary rescue probability can be approximated by

$$p_{\text{rescue}} \approx$$
$$\begin{cases} 1 - \exp\left[-\frac{u\lambda_a}{|\Delta_w|} \cdot \frac{v\lambda_w}{|\Delta_a|} \cdot \frac{\Delta_m}{\lambda_m} \cdot N\right], & \Delta_a T^* \ll -1, \\ 1 - \exp\left[-\frac{u\lambda_w}{|\Delta_w|} \cdot \sqrt{\frac{v\lambda_a \Delta_m}{\lambda_m}} \cdot N\right], & -1 \ll \Delta_a T^* \ll 1, \\ 1 - \exp\left[-\frac{u\lambda_w}{|\Delta_w|} \cdot \frac{\Delta_a}{\lambda_a} \cdot N\right], & 1 \ll \Delta_a T^*. \end{cases} \tag{18}$$

Appendix C: Evolutionary rescue time

We first calculate the expected time for the appearance of the first mutant that rescues the cell population. This can occur either through the evolutionary trajectory *wildtype* → *mutant* or through the trajectory *wildtype* → *aneuploid* → *mutant*. We start with the former.

Assuming no aneuploidy ($u = 0$), we define T_1 to be the time at which the first mutant cell appears that will avoid extinction and will therefore rescue the population. Note that if extinction occurs, that is the frequency of mutants after a very long time is zero, $m_\infty = 0$, then it is implied that $T_1 = \infty$, and vice versa if $T_1 < \infty$ then $m_\infty > 0$.

The number of successful mutants generated until time t can be approximated by an inhomogeneous Poisson process with rate $R_1(t) = v\lambda_w p_m w_t$, where $w_t = Ne^{\Delta_w t}$ is the number of wildtype cells at time t. Note that

$$\int_0^t R_1(z)\mathrm{d}z = v\lambda_w p_m N \frac{\exp[\Delta_w t] - 1}{\Delta_w} \approx v\lambda_w p_m N t, \tag{19}$$

by integrating the exponential and because $\frac{\exp[\Delta_w t]-1}{\Delta_w} = \frac{1+\Delta_w t+O(t^2)-1}{\Delta_w} = t + O(t^2)$. The probability density function of T_1 is thus $R_1(t) \exp\left(-\int_0^t R_1(z)\mathrm{d}z\right)$ (Allen, 2010). Therefore, the probability density function of the conditional random variable $(T_1 \mid T_1 < \infty)$ is $f_1(t) = \frac{R_1(t) \exp\left(-\int_0^t R_1(z)\mathrm{d}z\right)}{p_{\text{rescue}}}$.

We are interested in the mean conditional time, $\tau_1 = \mathbb{E}\left[T_1 \mid T_1 < \infty\right]$, which is given by

$$\tau_1 = \int_0^\infty t f_1(t)\mathrm{d}t = \frac{\int_0^\infty t R_1(t) \exp\left(-\int_0^t R_1(z)\mathrm{d}z\right)\mathrm{d}t}{p_{rescue}}, \tag{20}$$

Therefore, plugging eqs. (19) and (2) in eq. (20),

$$\tau_1 = \int_0^\infty t v\lambda_w N e^{\Delta_w t} \frac{e^{-v\lambda_w N p_m \frac{e^{\Delta_w t}-1}{\Delta_w}}}{1 - (1 - p_w)^N}\mathrm{d}t \approx \int_0^\infty t v\lambda_w N e^{\Delta_w t} \frac{e^{-v\lambda_w N p_m t}}{1 - e^{-N p_w}}\mathrm{d}t. \tag{21}$$

Figure 10B show the agreement between this approximating and simulation results.

When $Nu\lambda_w/|\Delta_w| \gg 1$ the aneuploid frequency dynamics is roughly deterministic and therefore can be approximated by

$$a_t \approx \frac{Nu\lambda_w e^{\Delta_w t}}{\Delta_w - \Delta_a}\left[1 - e^{-(\Delta_w - \Delta_a)t}\right]. \tag{22}$$

As a result, the number of successful mutants created by direct mutation and via aneuploidy can be approximated by inhomogeneous Poisson processes with the rates

$$r_1(t) = v\lambda_a p_m \int_0^t a_z \mathrm{d}z = \frac{uv\lambda_w\lambda_a N p_m}{\Delta_w - \Delta_a}\left(\frac{e^{\Delta_w t} - 1}{\Delta_w} - \frac{e^{\Delta_a t} - 1}{\Delta_a}\right), \tag{23}$$

$$r_2(t) = v\lambda_w p_m \int_0^t w_z \mathrm{d}z = v\lambda_w N p_m \frac{e^{\Delta_w t} - 1}{\Delta_w}. \tag{24}$$

For large initial population sizes we assume that the two processes are independent and as a result, they can be merged into a single Poisson process with rate $R_2(t) = (r_1 + r_2)(t)$. Consequently, the mean time to the appearance of the first rescue mutant is

$$\tau_2 = \frac{\int_0^\infty t R_2(t)\exp\left(-\int_0^t R_2(z)\mathrm{d}z\right)\mathrm{d}t}{p_{rescue}}$$

$$= \int_0^\infty t\left(v\lambda_a p_m a_t + v\lambda_w p_m w_t\right)\frac{\exp\left[-\frac{uv\lambda_w\lambda_a N p_m}{\Delta_w - \Delta_a}\left(\frac{e^{\Delta_w t} - 1}{\Delta_w} - \frac{e^{\Delta_a t} - 1}{\Delta_a}\right) - v\lambda_w N p_m\frac{e^{\Delta_w t} - 1}{\Delta_w}\right]}{1 - e^{-Np_w}}\mathrm{d}t, \tag{25}$$

which we plot in Figure 10A as a function of the initial population size, N.

Appendix D: Recurrence time

We define the proliferation time τ_2^r to be the time it takes the population of mutant cancer cells to reach the initial tumor size N. The number of rescue lineages generated by the wildtype population is given by eq. (23) (see Figure 11):

$$r_1(\infty) = \frac{uv\lambda_w\lambda_a N p_m}{|\Delta_w||\Delta_a|},$$

where we ignore lineages created by direct mutation because we assumed $u\lambda_a > \max(-\Delta_a, 1/T^*)$.

This helps us distinguish between two cases for the proliferation time. Firstly, when we have at most one lineages which rescues the cancer cell population:

$$N \ll \frac{|\Delta_w||\Delta_a|}{uv\lambda_w\lambda_a p_m}.$$

As a result, the recurrence time is given by (Avanzini and Antal, 2019):

$$\tau_2^r \approx \tau_2 + \frac{\log p_m N}{\Delta_m}. \tag{26}$$

The factor of p_m in the second term of eq. (26) is due to the fact that the lineage is conditioned to survive genetic drift and the time to reach N is shorter then the case without this property.

The second case is when the wildtype population produces a large number of rescue lineages in a short period of time. This is given by the condition:

$$N \gg \frac{|\Delta_w||\Delta_a|}{uv\lambda_w\lambda_a p_m}.$$

As a result, the recurrence time is obtained by solving the following system of ODEs:

$$\frac{dw}{dt} = \Delta_w w,$$
$$\frac{da}{dt} = \Delta_a a + u\lambda_w w, \tag{27}$$
$$\frac{dm}{dt} = \Delta_m m + v\lambda_a a + v\lambda_w w.$$

Solving the system of ODEs for initial condition $\left(w(0), a(0), m(0)\right) = (N, 0, 0)$ we obtain:

$$m(t) = \frac{Nuv\lambda_a\lambda_w}{\Delta_w - \Delta_a}\left[\frac{e^{\Delta_w t} - e^{\Delta_m t}}{\Delta_w - \Delta_m} - \frac{e^{\Delta_a t} - e^{\Delta_m t}}{\Delta_a - \Delta_m}\right] + Nv\lambda_w\frac{e^{\Delta_w t} - e^{\Delta_m t}}{\Delta_w - \Delta_m}.$$

We obtain τ_2^r such that $m\left(\tau_2^r\right) = N$ by solving:

$$1 = \frac{uv\lambda_a\lambda_w}{\Delta_w - \Delta_a}\left[\frac{e^{\Delta_w \tau_2^r} - e^{\Delta_m \tau_2^r}}{\Delta_w - \Delta_m} - \frac{e^{\Delta_a \tau_2^r} - e^{\Delta_m \tau_2^r}}{\Delta_a - \Delta_m}\right] + v\lambda_w\frac{e^{\Delta_w \tau_2^r} - e^{\Delta_m \tau_2^r}}{\Delta_w - \Delta_m}. \tag{28}$$

This is a transcendental equation which cannot be solved analytically but can solved numerically using one of the root solver algorithm in **Python**.

Appendix E: Distribution of evolutionary rescue time

The probability that a successful mutant has been generated by time t is given by:

$$P(rescue, t) = P(T_2 < t)$$
$$= 1 - \exp\left\{-\left[r_1(t) + r_2(t)\right]\right\}$$
$$= 1 - \exp\left\{-\left[\frac{uv\lambda_w\lambda_a Np_m}{\Delta_w - \Delta_a}\left(\frac{e^{\Delta_w t} - 1}{\Delta_w} - \frac{e^{\Delta_a t} - 1}{\Delta_a}\right) + v\lambda_w Np_m\frac{e^{\Delta_w t} - 1}{\Delta_w}\right]\right\},$$

where T_2 is the time at which the first mutant cell appears that will avoid extinction and which was defined in Appendix C.

As a result, the probability that a successful mutant has not been generated by time t is:

$$1 - P(rescue, t) = \exp\left\{-\left[\frac{uv\lambda_w\lambda_a Np_m}{\Delta_w - \Delta_a}\left(\frac{e^{\Delta_w t} - 1}{\Delta_w} - \frac{e^{\Delta_a t} - 1}{\Delta_a}\right) + v\lambda_w Np_m\frac{e^{\Delta_w t} - 1}{\Delta_w}\right]\right\}. \tag{29}$$

Appendix F: Distribution of recurrence time

The probability distribution of the time that a lineage, consisting initially of a single cell, will reach size N as time t is given by the Gumbel distribution $\text{Gumb}_{max}\left(\frac{\log Np_m}{\Delta_m}, \frac{1}{\Delta_m}\right)$ (Avanzini and Antal, 2019) with probability density function:

$$G(t) = e^{-p_m N e^{-\Delta_m t}}.$$

A mutant lineage initiated at time s, through aneuploidy, at rate $v\lambda_a p_m a_s$ reaches size N before time t with probability $G(t-s)$ where $s \leq t$. As a result, the number of successful mutant lineages which reach size N by time t can be approximated by inhomogeneous Poisson random variable with rate:

$$r(t) = v\lambda_a p_m \int_0^t a_s G(t-s) \, ds$$

where a_t is aneuploid population size at time t defined in eq. (22). The proliferation time is defined as the first time the size of all lineages reaches N. When $N \ll |\Delta_w||\Delta_a|/uv\lambda_w\lambda_a p_m$ there is at most a single mutant lineage that will survive and reach size N (Figure 11) and the probability that the size of that lineage has not reached N by time t is given by:

$$\begin{aligned}
P(m_t \leq N) &= 1 - P(\tau > t) = \exp\left[-r(t)\right] \\
&= \frac{Nuv\lambda_w\lambda_a p_m}{\Delta_w - \Delta_a} \int_0^t \left[e^{\Delta_w t} - e^{\Delta_a t}\right] e^{-p_m N e^{-\Delta_m(t-s)}} \, ds.
\end{aligned} \tag{30}$$

When $N \gg |\Delta_w||\Delta_a|/uv\lambda_w\lambda_a p_m$ the dynamics of the cancer cell populations is deterministic and approximated by the system of ODEs shown in eq. (27). As a result, the size of the mutant cell population will always be below N until time τ_2^r and will always be greater after:

$$P(m_t \leq N) = 1 - H\left(t - \tau_2^r\right), \tag{31}$$

where $H(x)$ is the Heaviside function:

$$H(x) = \begin{cases} 0, & x < 0, \\ 1, & x \geq 0. \end{cases}$$

We plot eq. (30) and eq. (31) in Figure and compare with stochastic simulations and observe that our approximation are in agreement.

We observe that for $N = 10^7$ our formula overestimates the probability that the mutant population will be smaller then N at time t. This can be explained by the fact that $N = 10^7$ is an intermediary case where the wildtype population produces a number of rescue lineages that is greater then one but still sufficiently small such that stochasticity plays an important role in the population dynamics. As a result, the number of mutant cancer cells will reach N faster then the case with a single mutant lineage.

Appendix F: Figures

A

B
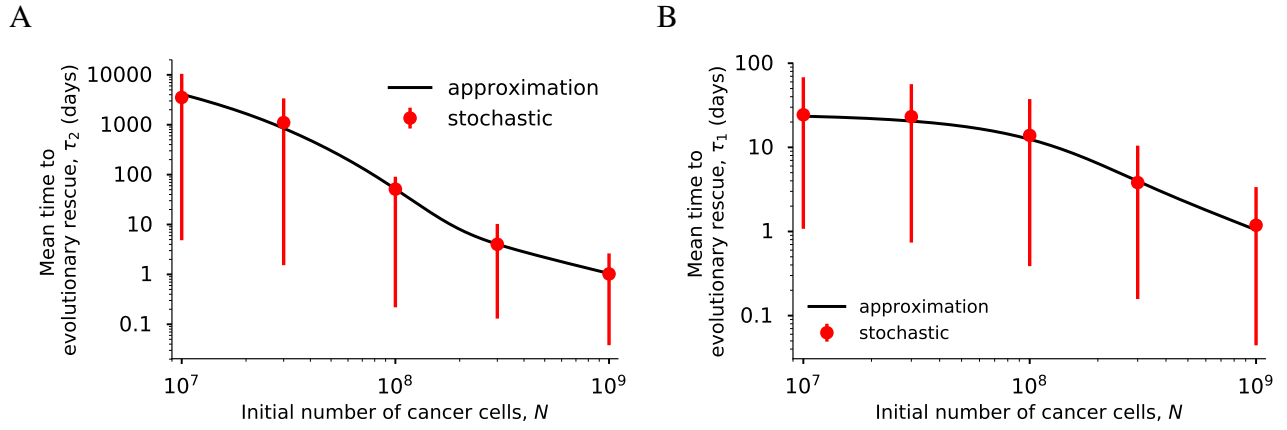
Figure 10: Evolutionary rescue time. Shown is the mean time for appearance of a resistance mutation the leads to evolutionary rescue **(left)** with aneuploidy ($u > 0$) and **(right)** without aneuploidy ($u = 0$). Our inhomogeneous Poisson-process approximations (solid black lines, right: eq. (20), left: eq. (25)) is in agreement with simulation results (red markers with 95% quantile intervals). Parameters: $\lambda_w = 0.1, \lambda_m = 0.0899, \lambda_m = 0.1, \mu_w = 0.14, \mu_a = 0.09, \mu_m = 0.09, u = 10^{-2}, v = 10^{-7}$.
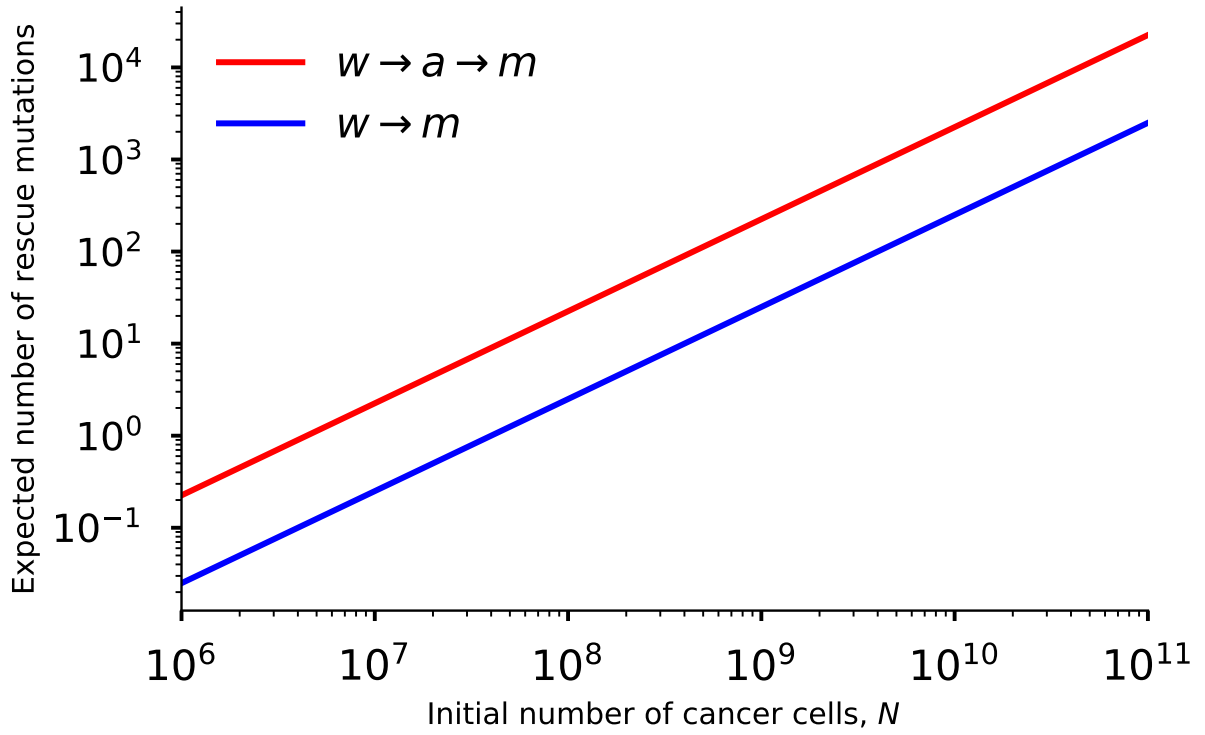
Figure 11: Aneuploidy increases the number of mutations which rescue the tumor. Shown is the expected number of mutation, which will rescue the cancer cell population, produced through the evolutionary trajectory *wildtype* → *mutant* (blue line, eq. (24)) or through the trajectory *wildtype* → *aneuploid* → *mutant* (red line, eq. (23)). Parameters: $\lambda_w = 0.1, \lambda_m = 0.0899, \lambda_m = 0.1, \mu_w = 0.14, \mu_a = 0.09, \mu_m = 0.09, u = 10^{-2}, v = 10^{-7}$.